PERFORMANCE ASSESSMENT OF GRATE INLETS FOR HIGHWAY MEDIAN DRAINAGE

Prepared for

The Urban Drainage and Flood Control District

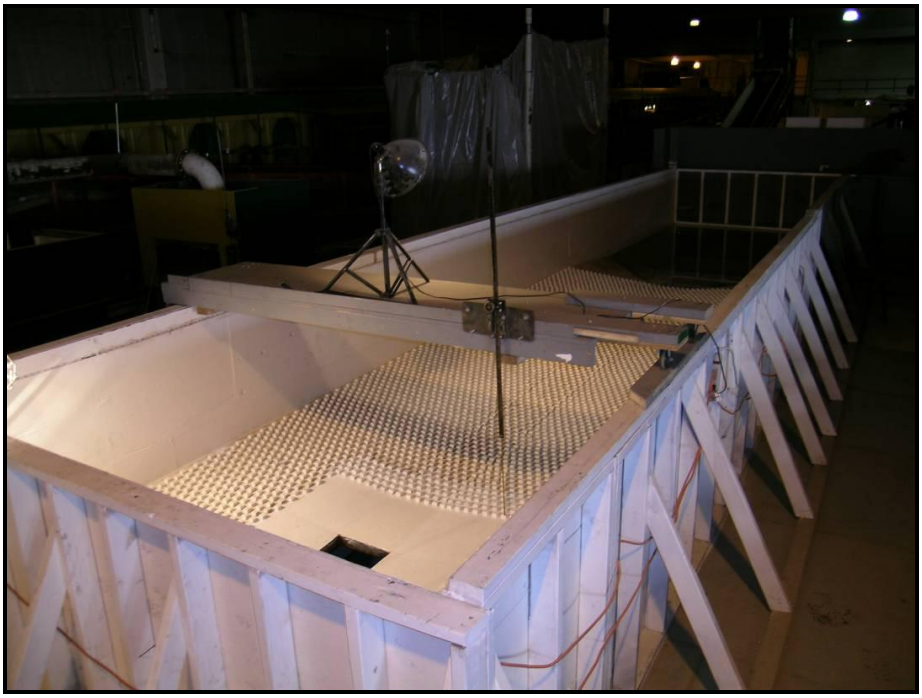

Prepared by

Brendan C. Comport
Amanda L. Cox
Christopher I. Thornton

April 2012

Colorado State University
Daryl B. Simons Building *at the*
Engineering Research Center
Fort Collins, CO 80523

Colorado State University

PERFORMANCE ASSESSMENT OF GRATE INLETS FOR HIGHWAY MEDIAN DRAINAGE

Prepared for

The Urban Drainage and Flood Control District

Prepared by

Brendan C. Comport
Amanda L. Cox
Christopher I. Thornton

April 2012

Colorado State University
Daryl B. Simons Building *at the*
Engineering Research Center
Fort Collins, CO 80523

Colorado State University

TABLE OF CONTENTS

LIST OF FIGURES

LIST OF TABLES

LIST OF SYMBOLS, UNITS OF MEASURE, AND ABBREVIATIONS

Symbols

H	head above the inlet (ft)
L_r	length, width, and depth (geometry)
n	Manning's roughness
n_r	Manning's roughness scaling ratio (dynamics)
Q	volumetric flow rate or theoretical volumetric flow rate (cfs)
Q_r	discharge (kinematics)
V_r	velocity (kinematics)
ρ_r	fluid density (dynamics)

Units of Measure

cfs	cubic feet per second
º, deg	degree(s), as a measure of angular distance
ft	feet or foot
ft^2	square feet
hp	horse power
in.	inch(es)
%	percent

Abbreviations

BMP	Best Management Practice
CDOT	Colorado Department of Transportation
CSU	Colorado State University
ERC	Engineering Research Center
ID	identification
Mag meter	electro-magnetic flow meter
QC	quality control
®	registered
™	trademark
Type C	CDOT single grate inlet tested at CSU

Type D	CDOT double grate inlet tested at CSU
UDFCD	Urban Drainage and Flood Control District
USBR	U. S. Bureau of Reclamation
USDCM	*Urban Storm Drainage Criteria Manual*

1 INTRODUCTION

A research program was conducted at Colorado State University (CSU) to evaluate the performance of two highway median storm drain inlets. Inlets tested in this study are currently used by the Urban Drainage and Flood Control District (UDFCD) of Denver, and consist of the Colorado Department of Transportation Type C and D configurations. The Type C and D inlets have not previously been studied or tested for development of performance equations. Current design practices are based upon general application of the orifice and/or weir equations. The study presented in this report focused on collecting data on Type C and D inlets under physically-relevant design conditions for analysis by the UDFCD. A 3:1 Froude-scale model of a highway median was designed and built at the Engineering Research Center (ERC) of CSU. The model consisted of a constructed highway median channel with one interchangeable inlet. A total of 120 hydraulic tests including twenty-four debris tests were performed. Details pertaining to model construction, testing procedure, and resulting database are presented in this report.

1.1 Project Background

Storm-water runoff is typically conveyed across highway road surfaces and into a center median where it drains through inlets. Storm-water management in the metropolitan Denver area falls under the jurisdiction of the UDFCD. Policies, design procedures, and Best Management Practices (BMPs) are provided in the "*Urban Storm Drainage Criteria Manual*" (*USDCM*; UDFCD, 2008). Design methods presented in the *USDCM* for determining inlet efficiency provide the currently accepted methodology for design of storm-water collection systems throughout the region depicted in Figure 1-1. Guidance is provided in the *USDCM* for local jurisdictions, developers, contractors, and industrial and commercial operations in selecting, designing, maintaining, and carrying-out BMPs to effectively handle storm-water runoff

(UDFCD, 2008). Other agencies participating in this study included the University of Colorado at Denver and the Colorado Department of Transportation (CDOT).

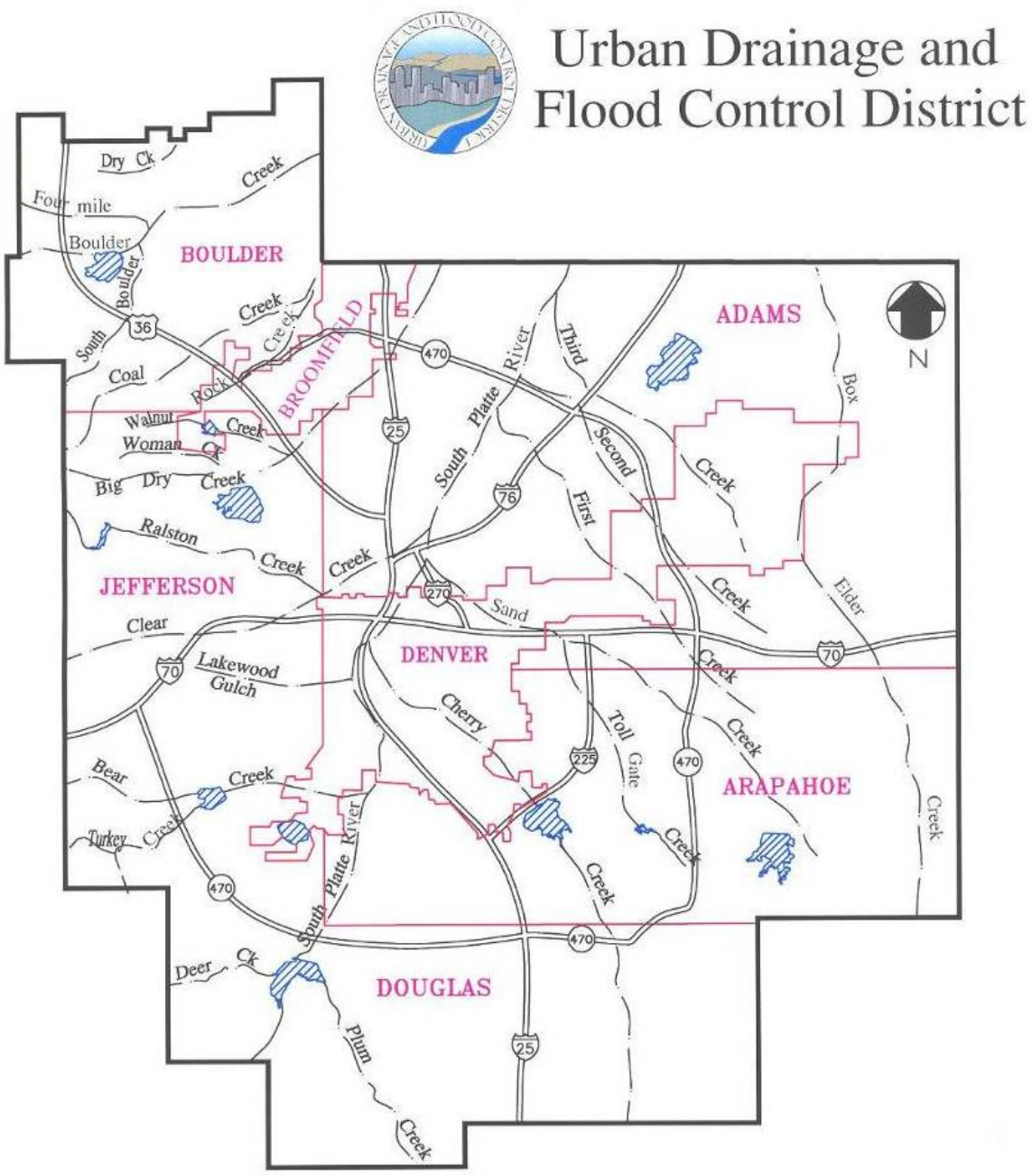

Figure 1-1: Map of the Urban Drainage and Flood Control District (UDFCD, 2008)

The need for the median inlet study stemmed from uncertainty in selecting appropriate discharge coefficients for the Type C and D inlets for use in the weir and/or orifice equations.

Local jurisdictions depicted in Figure 1-1 often utilize the Type C and D inlets for highway drainage. Uncertainties in sizing the inlets and in the level of flood protection afforded were realized. Uncertainty in design practice can lead to over-design and wasted expense. Therefore, a need was identified for greater accuracy in design for the Type C and D inlets. Results of this research program are intended to be used to supplement the *USDCM* design methodology.

1.2 Research Objectives

A testing program was developed by the UDFCD to produce sufficient data for development of discharge coefficients for use in the orifice equation.

Objectives of this project were:

- to construct a 3:1 Froude-scale model of a highway median with an interchangeable inlet;
- to conduct hydraulic tests for multiple inlet configurations and grate angles where stage-discharge data are collected; and
- to conduct a debris test for each inlet configuration and provide a qualitative assessment of the effect of debris on the inlet efficiency and overall performance.

1.3 Report Organization

This report presents the project background and research objectives, description of the test facility and model fabrication, test data, and conclusions. Included with the report is a CD that contains the Microsoft Word® (.doc) and Adobe® Acrobat® (.pdf) report files, along with the Microsoft Excel® (.xls) spreadsheet data files. Also provided to the UDFCD with this report is an Electronic Data Supplement (stored on a DVD) that contains the CD contents and all test data and photographic documentation. The reader is referred to the UDFCD for obtaining photographs and video documentation.

2 HYDRAULIC MODELING

A physical model was designed and constructed which served to represent common field conditions. Testing was performed on the Type C and D inlets from September 2009 through June 2010. A total of 120 tests were performed where data collection focused on inlet flow depth and volumetric flow rate. This chapter details the testing facility, model construction, test conditions, and testing procedures.

2.1 Testing Facility Description and Model Scaling

Model construction and testing was performed at the ERC of CSU. A photograph of the flume, pipe network, and drainage facilities is presented in Figure 2-1. The model consisted of a headbox to supply water, a flume section containing the highway median section and inlets, supporting pumps, piping, several flow-measurement devices, a tailbox to capture returning flow, and the supporting superstructure.

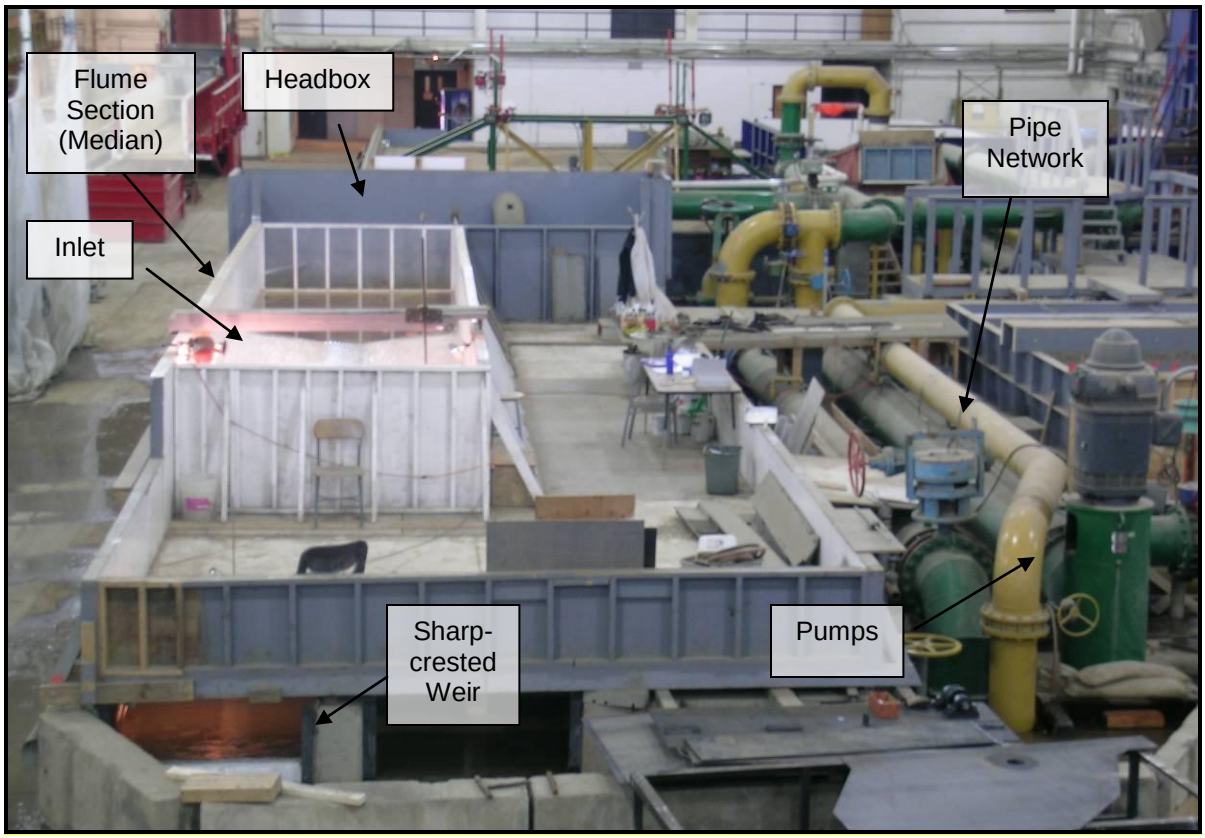

Figure 2-1: Photograph of model layout

Contained within the flume section were the highway median surface and all inlet components. The median section was constructed as a 2-in. by 4 in. (2x4) tubular steel framework and decked with 1/8-in. thick sheet steel. Upstream of the median section, a horizontal approach section was constructed to allow flow to become fully developed before the test section. A diffuser screen was installed at the junction between the headbox and the approach section to minimize turbulence and to distribute flow evenly across the width of the model. Prototype dimensions and characteristics are presented in Table 2-1.

Table 2-1: Prototype dimensions

Feature	Prototype Design
Scale (prototype:model)	3:1
Channel length (ft)	64
Channel width (ft)	24
Channel side slopes (%)	10
Channel longitudinal slope (%)	1.35
Approach section length (ft)	42
Downstream back slope (%)	10
Side slopes at inlet (%)	10
Average Manning's roughness	0.037
Surface material	1/8-in. steel plate
Inflow control	butterfly valve / diffuser screen
Inflow measurement	electro-magnetic flow meter
Outflow measurement	weir / point gage
Grate opening area – single grate (ft^2)	5.9
Depth of flow (ft)	3

Use of an exact Froude-scale model was chosen for this study. Table 2-2 provides scaling ratios used in the model. An exact scale model is well-suited for modeling flow near hydraulic structures, and the x-y-z length-scale ratios are all equal (Julien, 2002). The length scaling ratio was selected to be 3 to 1 (prototype:model) based on available laboratory space and pump capacity.

Table 2-2: Scaling ratios for geometry, kinematics, and dynamics

Geometry	Scale Ratios
Length, width, and depth (L_r)	3.00
All slopes	1.00
Kinematics	**Scale Ratios**
Velocity (V_r)	1.73
Discharge (Q_r)	15.6
Dynamics	**Scale Ratios**
Fluid density (ρ_r)	1.00
Manning's roughness (n_r)	1.20

An analysis of the Manning's roughness coefficient was conducted for the model to create the scaled roughness of typical vegetation found in highway medians. Additionally, the immediate area around the inlet grate(s) was given the scaled roughness of concrete to simulate a

concrete pad typically used in application. Dimensions of the concrete pad for each inlet configuration are located in Appendix A. An average friction slope over the range of expected flows was used with Manning's equation to calculate a roughness value for each of these surfaces. Figure 2-2 and Figure 2-3 present the results of testing the concrete surface and the median channel surface, respectively. Roughness was established for the area around the inlet(s) by adding coarse sand to industrial enamel paint (at about 15% by weight) and painting the simulated concrete pad. Roughness was established for the median section channel by adding 1-in. by 1-in. blocks cut from 3/4-in. thick plywood. Over 3,000 blocks were affixed to the model surface to give a block density of approximately 15% by area. The pattern was comprised of blocks placed in-line laterally and staggered longitudinally. Figure 2-4 provides a photograph which includes both the median and concrete pad surfaces. An average Manning's roughness value of 0.013 was determined for the concrete pad, which corresponds to a prototype value of 0.0156. An average Manning's roughness value of 0.031 was determined for the median channel, which corresponds to a prototype value of 0.037.

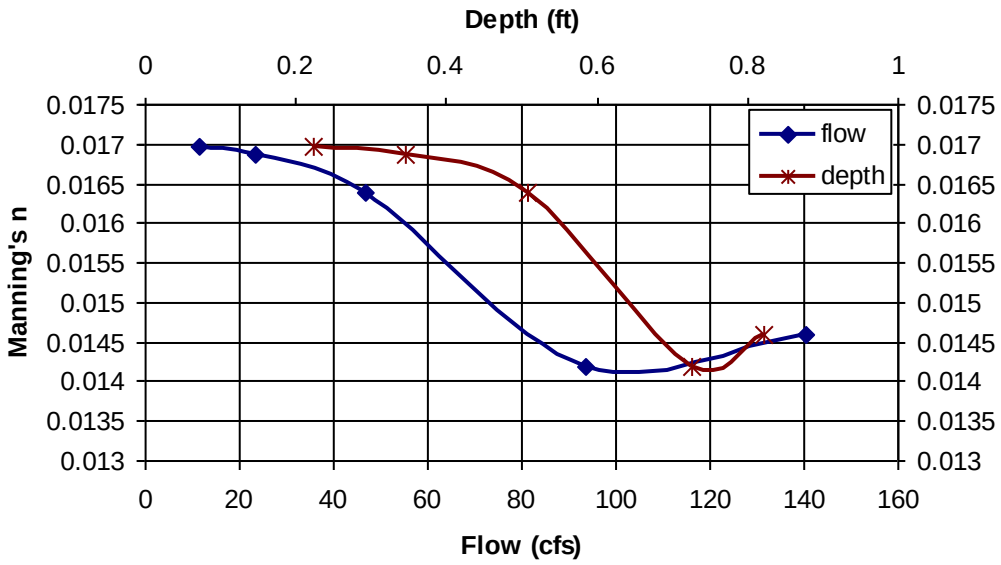

Figure 2-2: Manning's roughness for concrete pad (prototype)

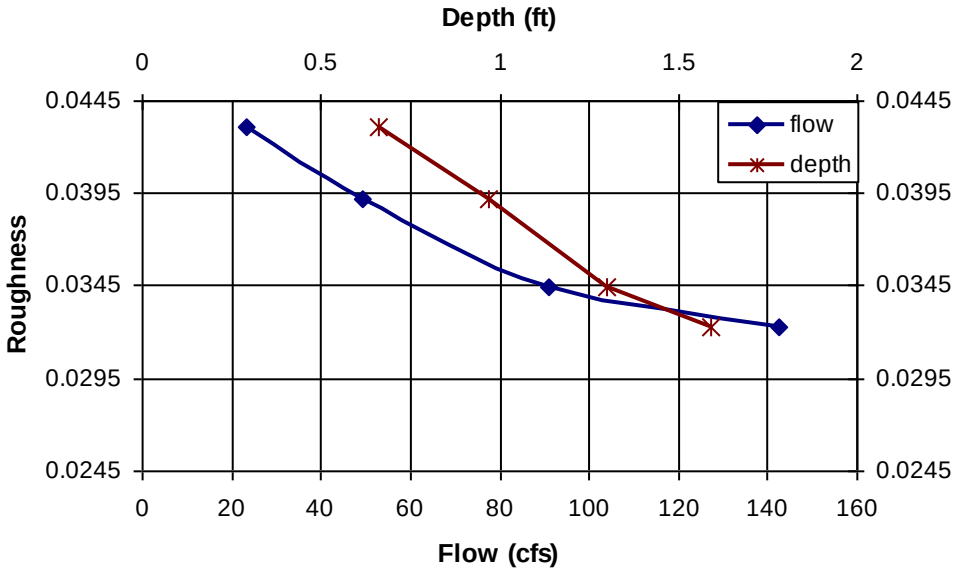

Figure 2-3: Manning's roughness for median channel (prototype)

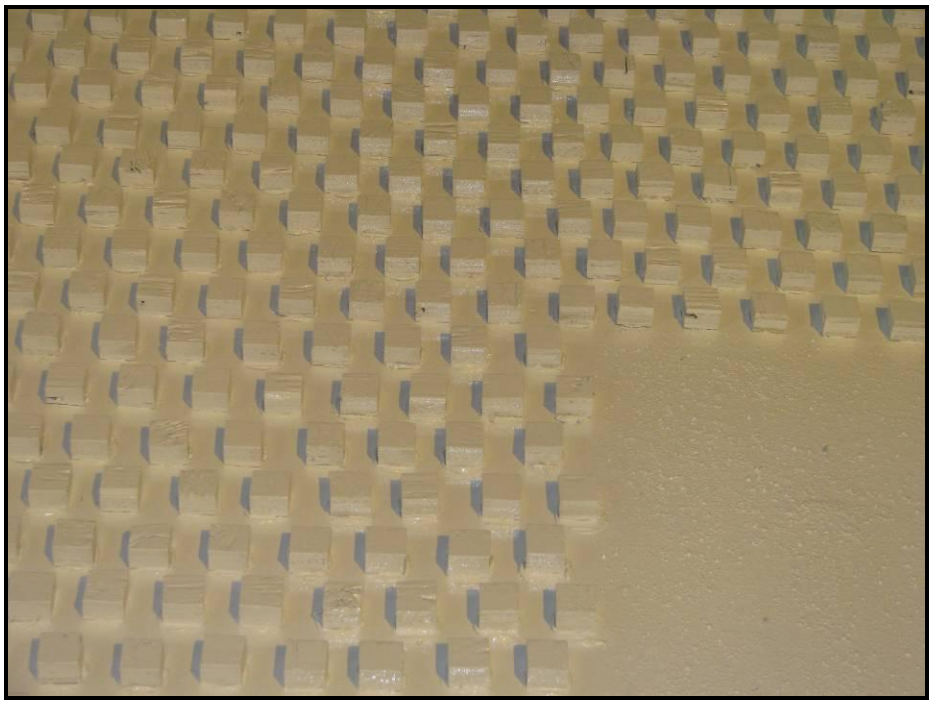

Figure 2-4: Surface roughness patterns

2.2 Inlet Configurations

One model was used for all inlet configurations. Only the area of the model around the grate(s) was re-constructed for each inlet configuration (*i.e.*, the simulated concrete pad and several rows of wood blocks). Inlet panels were fabricated from 1/8-in. thick sheet steel and grates were constructed of 1/8-in. thick aluminum plate. Angled supports were made at 10, 20, and 30 degrees from 1/8-in. thick sheet steel and fit to the inlet opening. The grate(s) were then fastened to the appropriate angled support and placed in the inlet opening when required. When angled grates were used in the on-grade configuration, the area around the grates was filled to the edge of the opening with gravel to provide a smooth transition. Sandbags were placed behind the inlets to simulate a small berm typically constructed in field application. Construction drawings of the model with each inlet type are presented in Appendix A. Photographs provided in Figure 2-5 through Figure 2-10 illustrate the inlet types and configurations.

(a) horizontal

(b) 10 degree

(c) 20 degree

(d) 30 degree

Figure 2-5: Type C inlet on-grade

(a) horizontal

(b) 10 degree (gravel not pictured)

(c) 20 degree (gravel not pictured)

(d) 30 degree (gravel not pictured)

Figure 2-6: Type C inlet depressed

(a) horizontal

(b) 10 degree

(c) 20 degree

(d) 30 degree

Figure 2-7: Type D inlet on-grade

(a) horizontal (grates not pictured)

(b) 10 degree

(c) 20 degree

(d) 30 degree

Figure 2-8: Type D inlet rotated

(a) horizontal

(b) 10 degree (gravel not pictured)

(c) 20 degree (gravel not pictured)

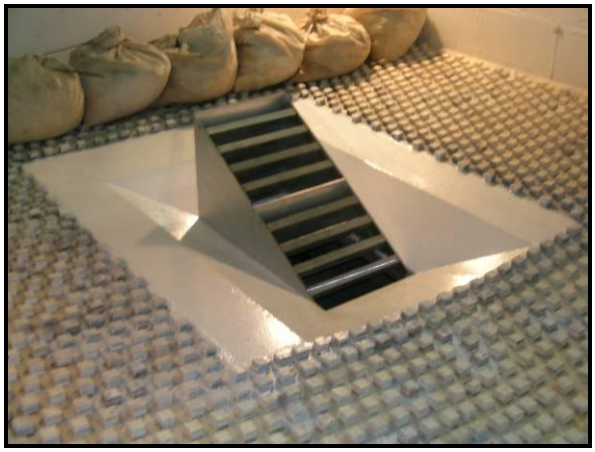

(d) 30 degree (gravel not pictured)

Figure 2-9: Type D inlet depressed

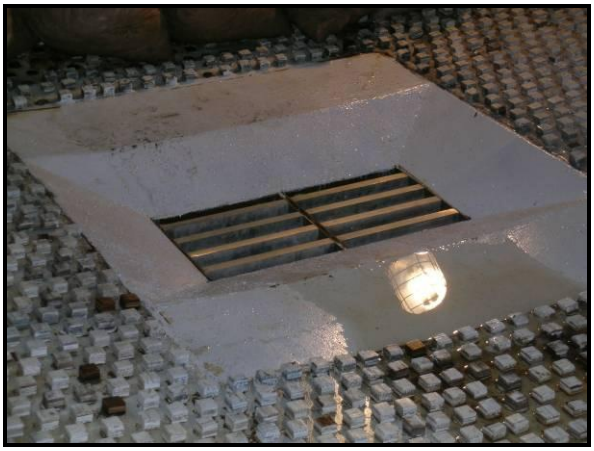

(a) horizontal

(b) 10 degree (gravel not pictured)

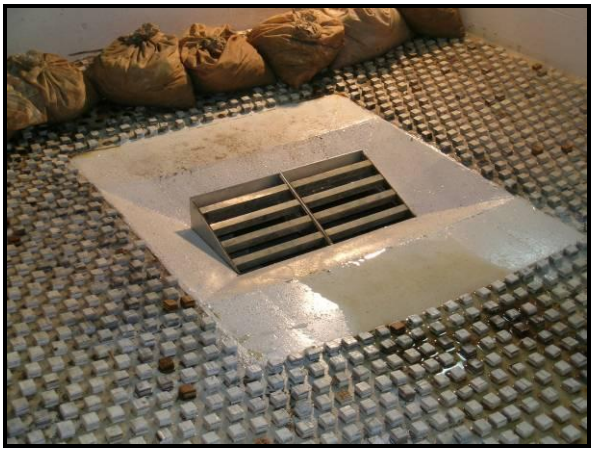

(c) 20 degree (gravel not pictured)

(d) 30 degree (gravel not pictured)

Figure 2-10: Type D inlet depressed and rotated

2.3 Conditions Tested

A test matrix was developed to organize the variation of parameters through all configurations. Target flow depths were provided by the UDFCD and typically consisted of 1-, 1.5-, 2.25-, and 3-ft depths at the prototype scale. Rationale for selection of these depths was based on a typical maximum design flow depth of 3 to 4 ft for highway medians. One grate design was used for both the Type C and D inlets. The Type C inlet consisted of a single grate and was used in on-grade and depressed configurations. The inlet was depressed approximately 4 in. below the existing grade for the depressed Type C configuration. The Type D inlet consisted of two grates configured laterally or in-line with the direction of flow. A depressed

Type D configuration was also used in which two grates were depressed approximately 4 in. below the existing grade. Tested flow depths for depressed grates were increased by 4 in. (1 prototype foot) to compensate for the depression and maintain consistent test conditions relative to the rest of the model. Each grate was positioned horizontally and at three angles, 10, 20 and 30 degrees, relative to the horizontal.

Several debris tests were also performed for the Type C and D inlets. A single piece of 1/4-in. thick plywood, with surface area equal to half the grate area, was introduced into the model and allowed to stick to the grate surface. Debris tests were performed for one flow depth per grate angle and inlet configuration. The flow depths used for debris testing were 1 ft for the non-depressed inlets and 2 ft for the depressed inlets. A total of 120 tests, including twenty-four debris tests, resulted from variations of inlet configurations, grate angles, and flow depths. Table 2-3 presents the test matrix completed during the study.

Table 2-3: Test matrix

(a) grate angle = 0 degree

Flow Depth (ft):	1	1.5	2.25	3	2	2.5	3.25	4	Other
Type C	1	1	1	1					
Type C – debris test	1								
Type C depressed					1	1	1	1	
Type C depressed – debris test					1				
Type D	1	1	1	1					
Type D – debris test	1								
Type D depressed					1	1	1	1	
Type D depressed – debris test					1				
Type D rotated	1	1	1	1					
Type D rotated – debris test	1								
Type D rotated depressed					1	1	1	1	
Type D rotated depressed – debris test					1				
Totals:	6	3	3	3	6	3	3	3	0

(b) grate angle = 10 degree

Flow Depth (ft):	1	1.5	2.25	3	2	2.5	3.25	4	Other
Type C	1	1	1	1					
Type C – debris test									1
Type C depressed					1	1	1	1	
Type C depressed – debris test									1
Type D	1	1	1	1					
Type D – debris test									1
Type D depressed					1	1	1	1	
Type D depressed – debris test									1
Type D rotated	1	1	1	1					
Type D rotated – debris test									1
Type D rotated depressed					1	1	1	1	
Type D rotated depressed – debris test									1
Totals:	3	3	3	3	3	3	3	3	6

(c) grate angle = 20 degree

Flow Depth (ft):	1	1.5	2.25	3	2	2.5	3.25	4	Other
Type C	1	1	1	1					
Type C – debris test									1
Type C depressed					1	1	1	1	
Type C depressed – debris test									1
Type D	1	1	1	1					
Type D – debris test									1
Type D depressed					1	1	1	1	
Type D depressed – debris test									1
Type D rotated	1	1	1	1					
Type D rotated – debris test									1
Type D rotated depressed					1	1	1	1	
Type D rotated depressed – debris test									1
Totals:	3	3	3	3	3	3	3	3	6

(d) grate angle = 30 degree

Flow Depth (ft):	1	1.5	2.25	3	2	2.5	3.25	4	Other
Type C	1	1	1	1					
Type C – debris test									1
Type C depressed					1	1	1	1	
Type C depressed – debris test									1
Type D	1	1	1	1					
Type D – debris test									1
Type D depressed					1	1	1	1	
Type D depressed – debris test									1
Type D rotated	1	1	1	1					
Type D rotated – debris test									1
Type D rotated depressed					1	1	1	1	
Type D rotated depressed – debris test									1
Totals:	3	3	3	3	3	3	3	3	6

2.4 Model Operation and Testing Procedures

Water was supplied from the sump to the model headbox by a 40-horsepower (hp) pump through a network of pipes and valves. Water flowed from the inlet valve to the headbox, through the flume section and inlets, and then exited into the sump beneath the model. All flow entering the model was captured by the inlets. Figure 2-11 provides a schematic of the entire model. A lined channel below the flume conveyed flow away from the inlet and back into the sump.

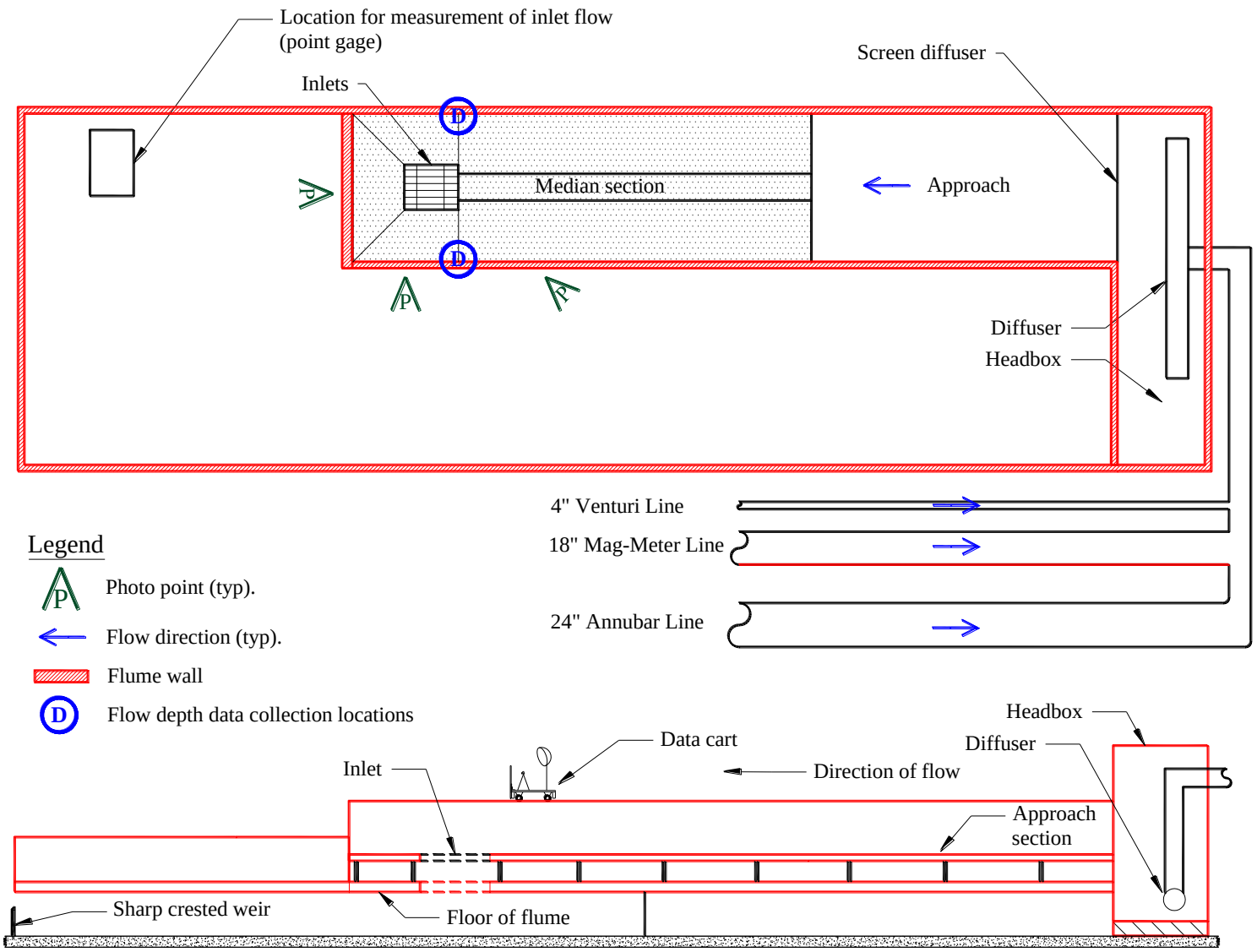

Figure 2-11: Model schematic

Flow entering and exiting the model was measured as part of the data-collection process. A full-bore electro-magnetic flow meter (Mag-meter) manufactured by the Endress and Hauser Company was used to measure inflow. Table 2-4 summarizes flow-measurement characteristics for the Mag-meter.

Table 2-4: Inflow measurement characteristics

Instrument Type	Flow Range (cfs)	Pipeline (in.)	Pump (hp)	Accuracy (%)
Mag-meter	0.13 - 10	18	40	0.5

Outflow from the channel below the model was measured by a rectangular sharp-crested weir. The weir was constructed in accordance with published specifications (USBR, 2001), and calibrated prior to testing. A rating equation was developed by regression analysis of flow-depth data over the expected operating range, and is given as Equation 2-1. An R-squared value of 0.994 was determined for the regression:

$$Q = 15.4H^{1.48} \qquad \textbf{Equation 2-1}$$

where:

Q = discharge (cfs); and

H = head above the weir crest (ft).

Flow depths for each test were measured at two locations, each lateral to the front edge of the grate(s) at the flume walls. The average of the two flow-depth readings was reported. The locations were chosen to be free of surface curvature from flow being drawn into the inlets and served as a control section to establish the depth and adjust the flow into the model for each test. Flow depth was measured using a point gage with ±0.001 ft accuracy, which was mounted on a data-collection cart designed to slide along the model and perform other water-surface measurements as well. Figure 2-12 provides a photograph of the data-collection cart. Three photograph taking and video recording locations were used for documentation: 1) an oblique view from adjacent to the data cart looking down at the inlets, 2) a view from directly behind the inlets looking upstream, and 3) a plan view from directly above the inlets.

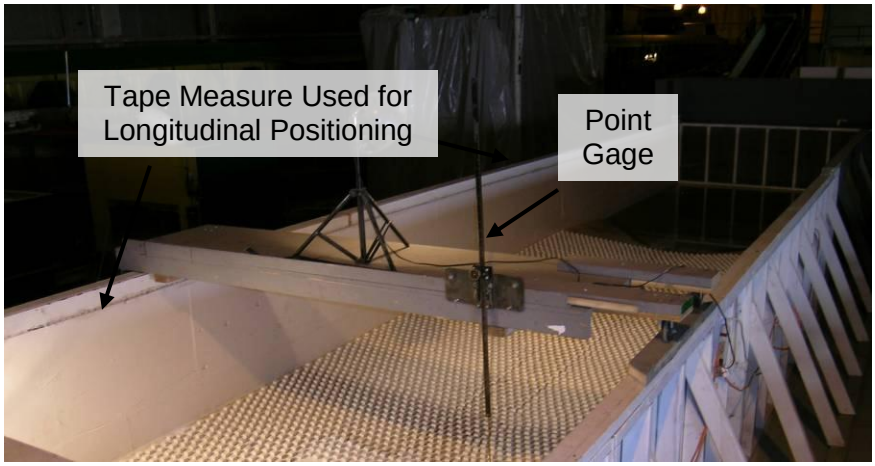

Figure 2-12: Data-collection cart photograph (looking upstream)

Following a standardized testing procedure assured consistency and facilitated data collection by multiple technicians. Prior to testing, the model was configured with the appropriate inlet and grate angle. The desired flow depth was set on the point gage and the flow into the model was adjusted to contact the point gage. The tolerance for achieving target flow depths was allowed to be 1 in. (or 3 prototype inches). Technicians waited approximately 10 minutes for flow conditions to stabilize once the depth was set. Outflow measurement point gages were checked periodically during this time until the readings stabilized. When flow into the model equaled outflow, indicating a steady-state condition, flow depth, discharge, and channel inundation extents were recorded and a qualitative description of the flow into the inlet was documented. Inundation extents were recorded by measuring the top width at every 1-ft longitudinal station. Fixed measuring tapes were used to determine lateral and longitudinal extents of water. Both tapes were graduated in tenths of a foot and had ±0.01 ft accuracy. Inundation data for each test are provided in the Electronic Data Supplement. A new flow depth was then set on the point gage and the flow adjusted accordingly for subsequent tests with the same grate angle. The pumps were shut off and the model was reconfigured for consecutive tests with different inlet configurations or grate angles.

Debris testing entailed a single piece of 1/4-in. plywood introduced into the model at the upstream end. Several trials were performed to determine patterns in debris behavior. Debris tended to stick to the grate in predictable locations (*i.e.*, top, middle, or bottom) for a given grate

angle and flow depth. Once the debris was introduced into the channel, the flow depth was allowed to stabilize and a new flow-depth reading was collected.

Data collection was documented by completing a data sheet for each test, taking still photographs, and recording short videos. The data-collection sheet used for all testing is presented in Appendix C. Data collection was comprised of the following information: date, operator name, water temperature, test ID number, start and end times, inlet configuration, depth of flow, extent of flow, and flow characteristics. Flow characteristics consisted of any general observations that the operator recorded for a particular test. Typical observations included the condition of flow around the inlets, magnitude of vortex formation, and patterns observed in debris behavior. Several measures were taken to maintain data quality. After the testing procedures described above were followed, data were entered into the database by the operator, and then checked by a second person for accuracy with the original data sheets. A survey of the model was performed every time the model inlet type was changed which confirmed that the model was not shifting or settling, and that the slope was accurate to within allowable limits of 0.05% for longitudinal and cross slopes.

3 DATA AND OBSERVATIONS

Results of testing presented in this report have been collected using the previously described test procedures and quality control (QC) measures, and are presented at the prototype scale. Appendix B provides resulting data from the hydraulic model testing. Data are presented in this section in graphical form, by inlet type, and qualitative observations are made concerning the performance of the Type C and D inlets. Figure 3-1 through Figure 3-6 provide the stage-discharge relationships for each inlet configuration. The entire collected data set is presented in tabular form in Appendix B, where it is organized by: test ID number, inlet configuration, depth, and flow.

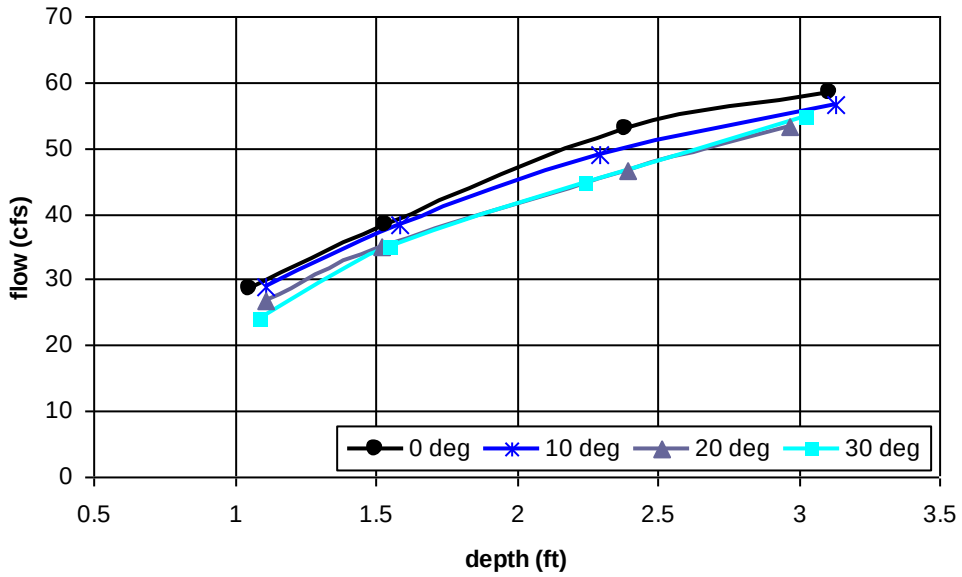

Figure 3-1: Type C inlet

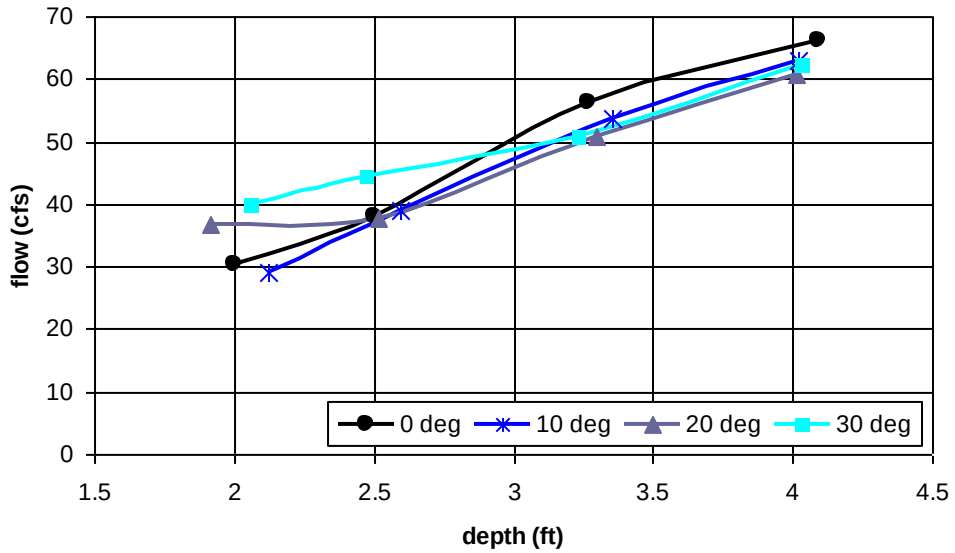

Figure 3-2: Type C inlet depressed

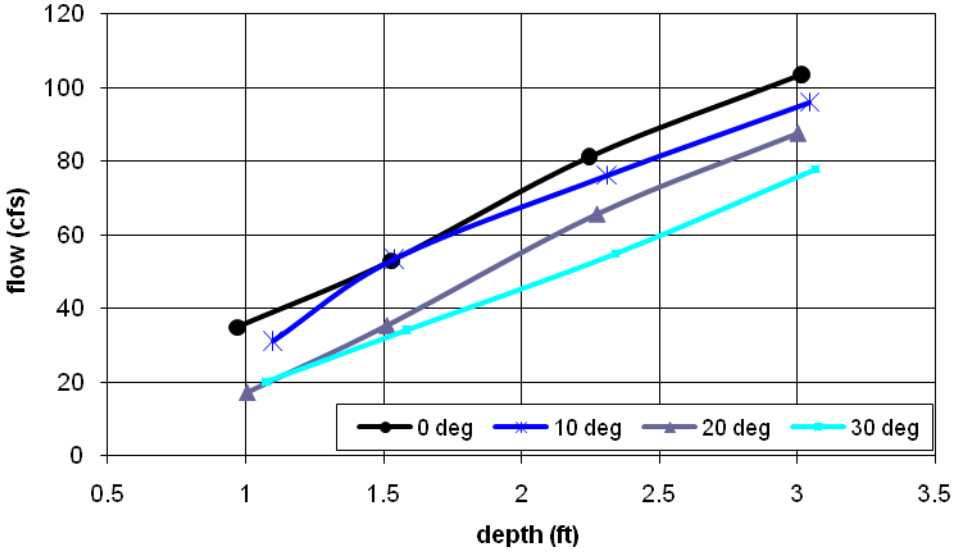

Figure 3-3: Type D inlet

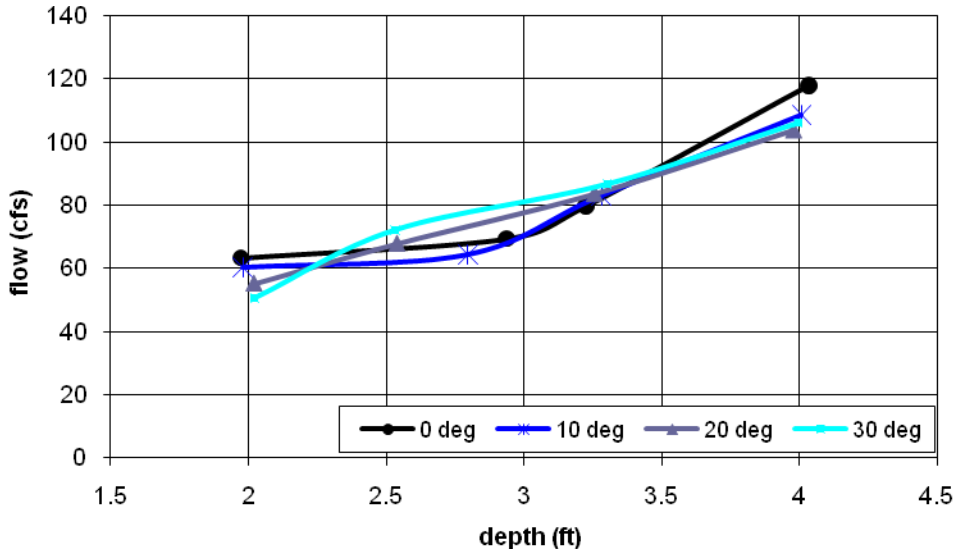

Figure 3-4: Type D inlet depressed

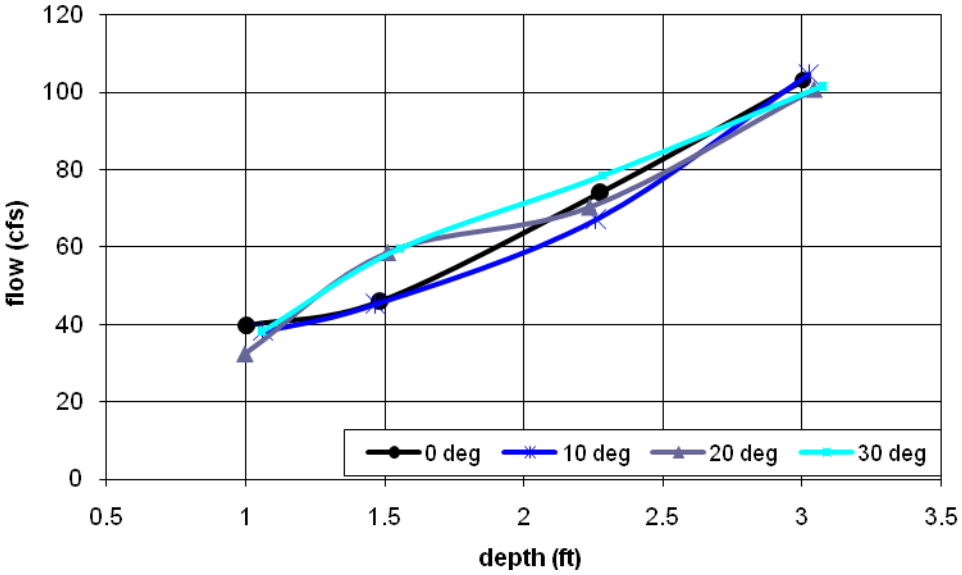

Figure 3-5: Type D inlet rotated

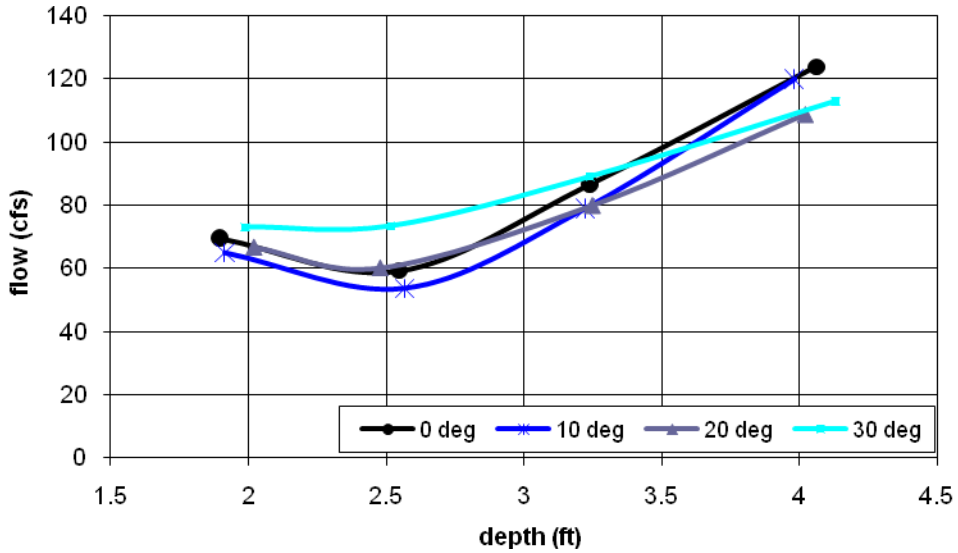

Figure 3-6: Type D inlet depressed and rotated

Several trends were observed during testing and in the test data:

- The stage-discharge relationship for a given inlet configuration was greatly affected by the magnitude of vortex formation. A larger vortex resulted in less flow passing for a given flow depth.
- Large changes in flow depth often resulted from small changes in flow when vortex formation occurred.
- As inlet angle increased, the flow through the inlet generally increased for a given flow depth.
- Debris tend to stick as high up a grate as the flow depth will allow (*i.e.*, at the water surface).
- After debris stick to a grate surface, flow depth typically increased due to the reduced flow area.
- For the 0- and 10-degree grate angles, the stage-discharge relationship often exhibited a convex curve shape commonly found with orifice flow.
- For the 20- and 30-degree grate angles, the stage-discharge relationship often exhibited a concave curve shape commonly found with weir flow.

4 SUMMARY

A research program was conducted at Colorado State University to evaluate the performance of the Colorado Department of Transportation Type C and D highway median storm drain inlets. A 3:1 Froude-scale model of a highway median was designed and constructed at the Engineering Research Center of CSU. The model consisted of a constructed highway median channel with one interchangeable inlet. A total of 120 hydraulic tests, including twenty-four debris tests, were conducted from September 2009 to June 2010. Variations in inlet configuration and grate angle were investigated to provide flow-depth and discharge data. Resulting stage-discharge data were tabulated and plotted, and several qualitative observations were reported regarding the hydraulic conditions during testing and debris assessments.

REFERENCES

Julien, P. Y. (2002). River Mechanics. New York, NY: Cambridge University Press.

U. S. Bureau of Reclamation (2001). Water Measurement Manual. Third Edition, U. S. Department of the Interior, Denver, CO.

Urban Drainage and Flood Control District (2008). Urban Storm Drainage Criteria Manual. Denver, CO.

APPENDIX A

GRATE AND INLET SCHEMATICS

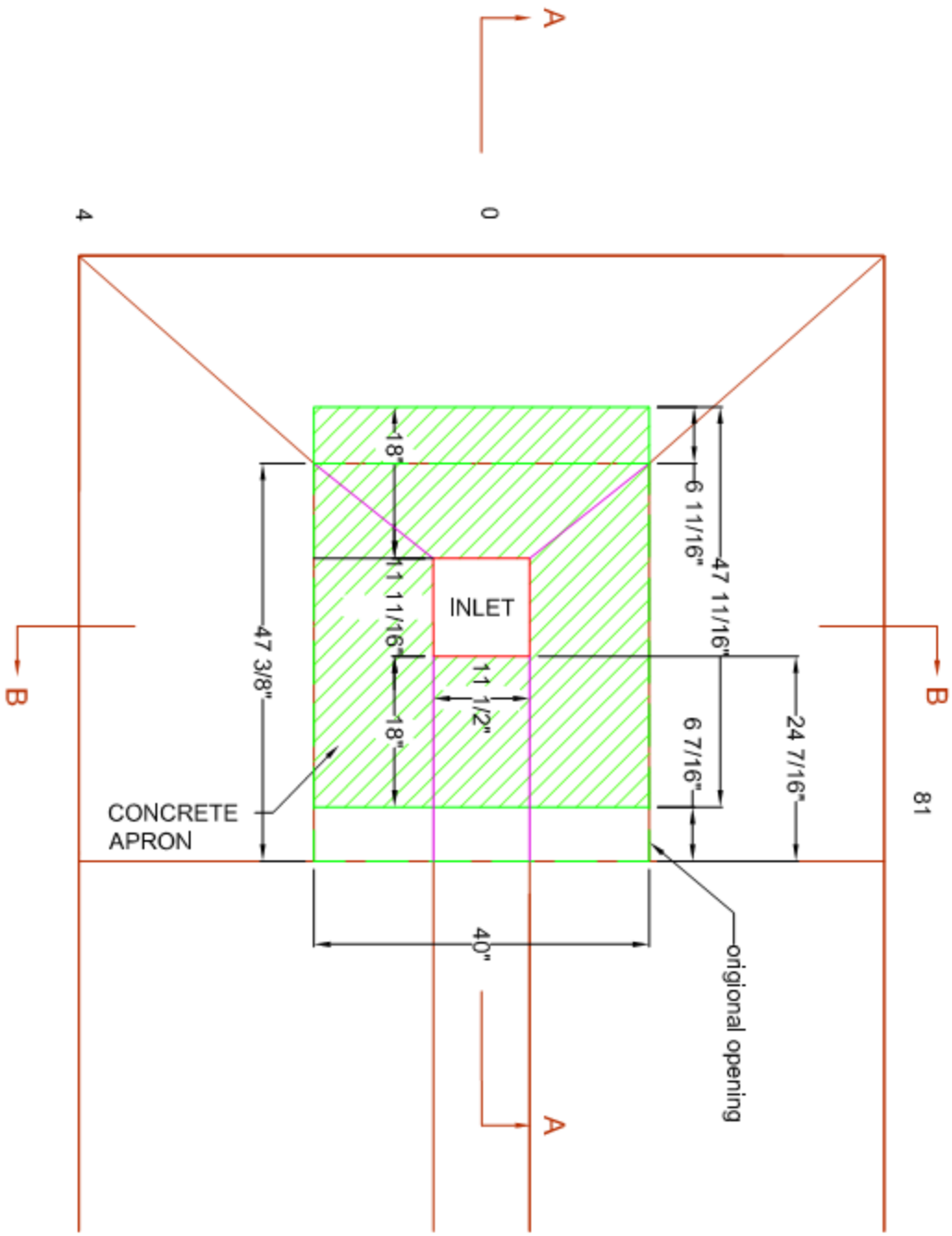

(a) plan view

Figure A-1: Type C inlet schematics

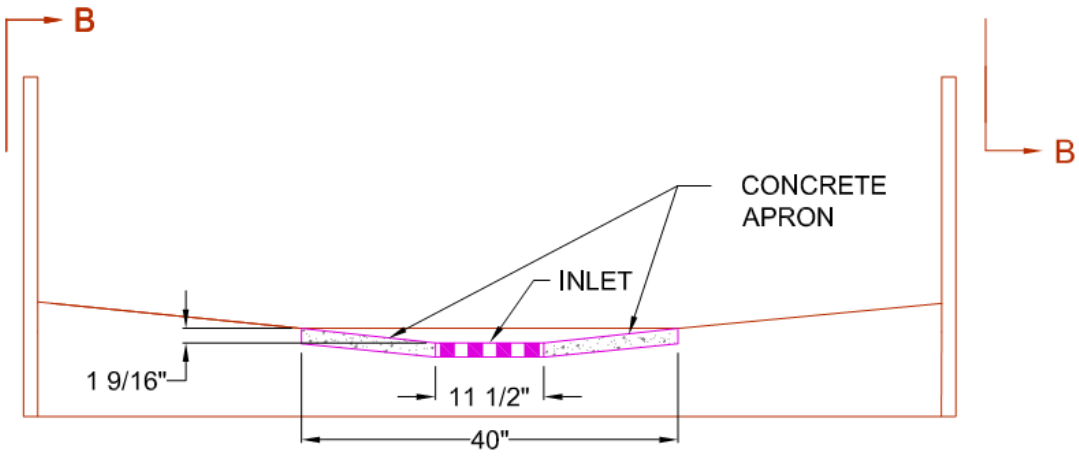

(b) Section B-B

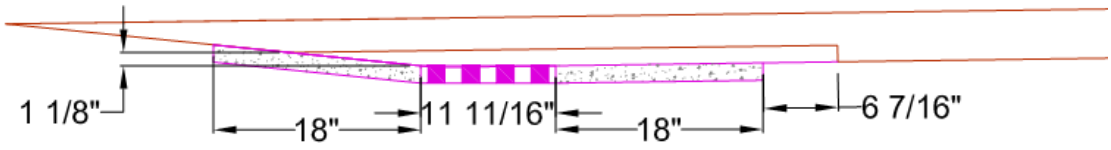

(c) Section A-A

Figure A-1 (continued): Type C inlet schematics

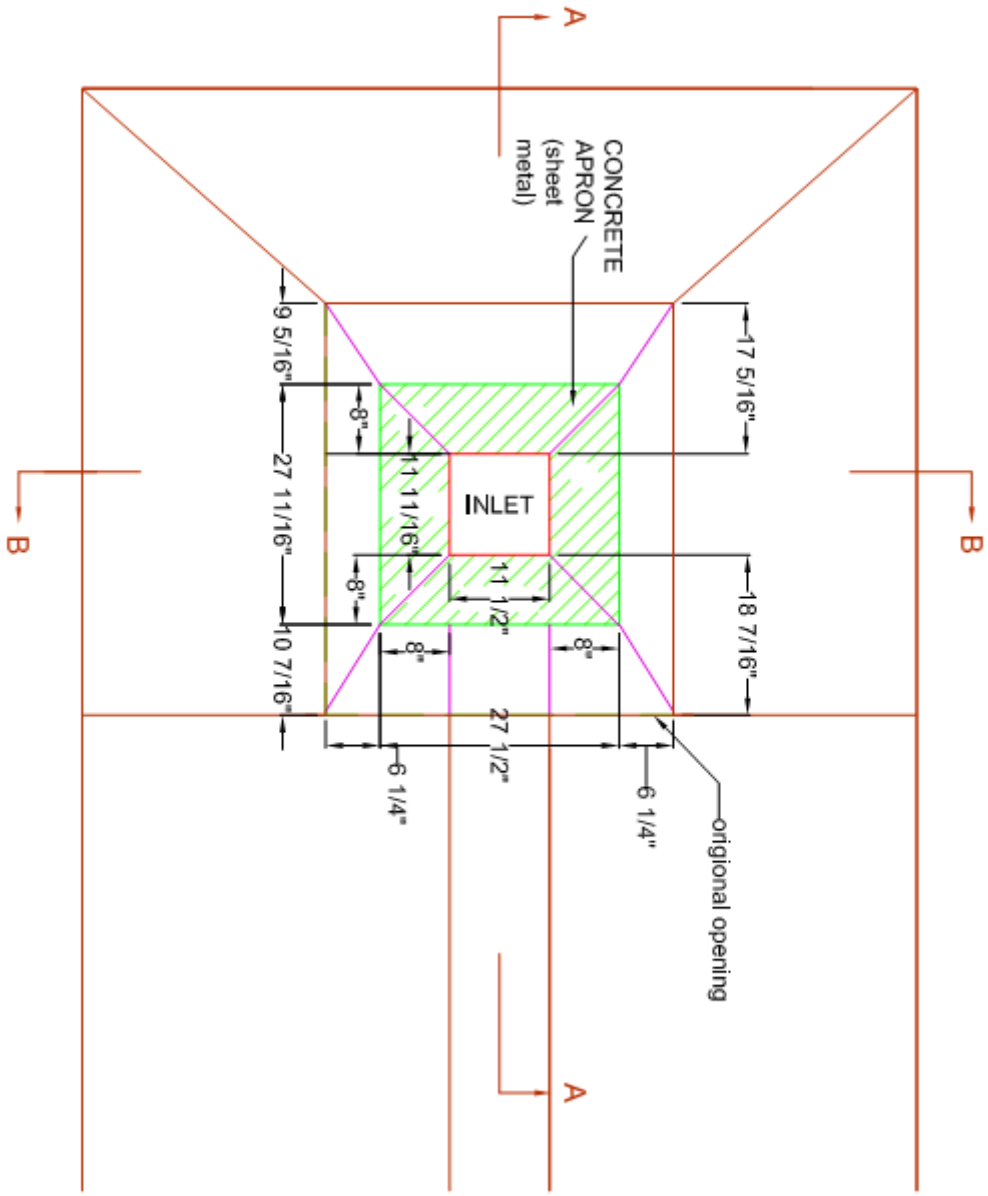

(a) plan view

Figure A-2: Type C inlet depressed schematics

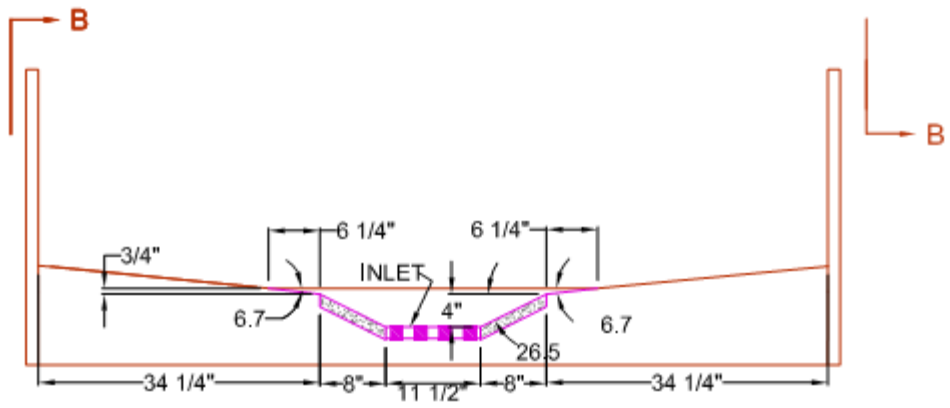

(b) Section B-B

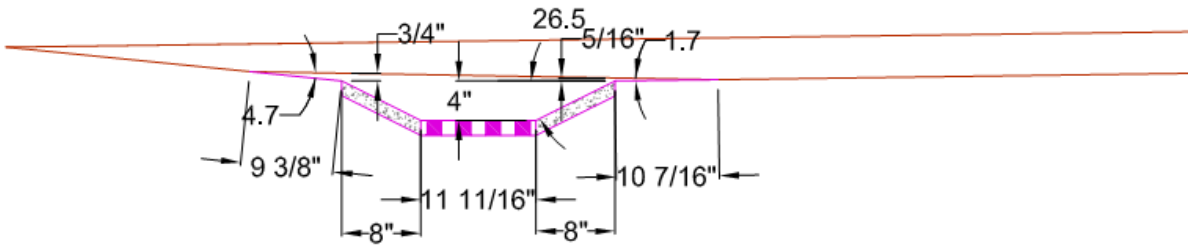

(c) Section A-A

Figure A-2 (continued): Type C inlet depressed schematics

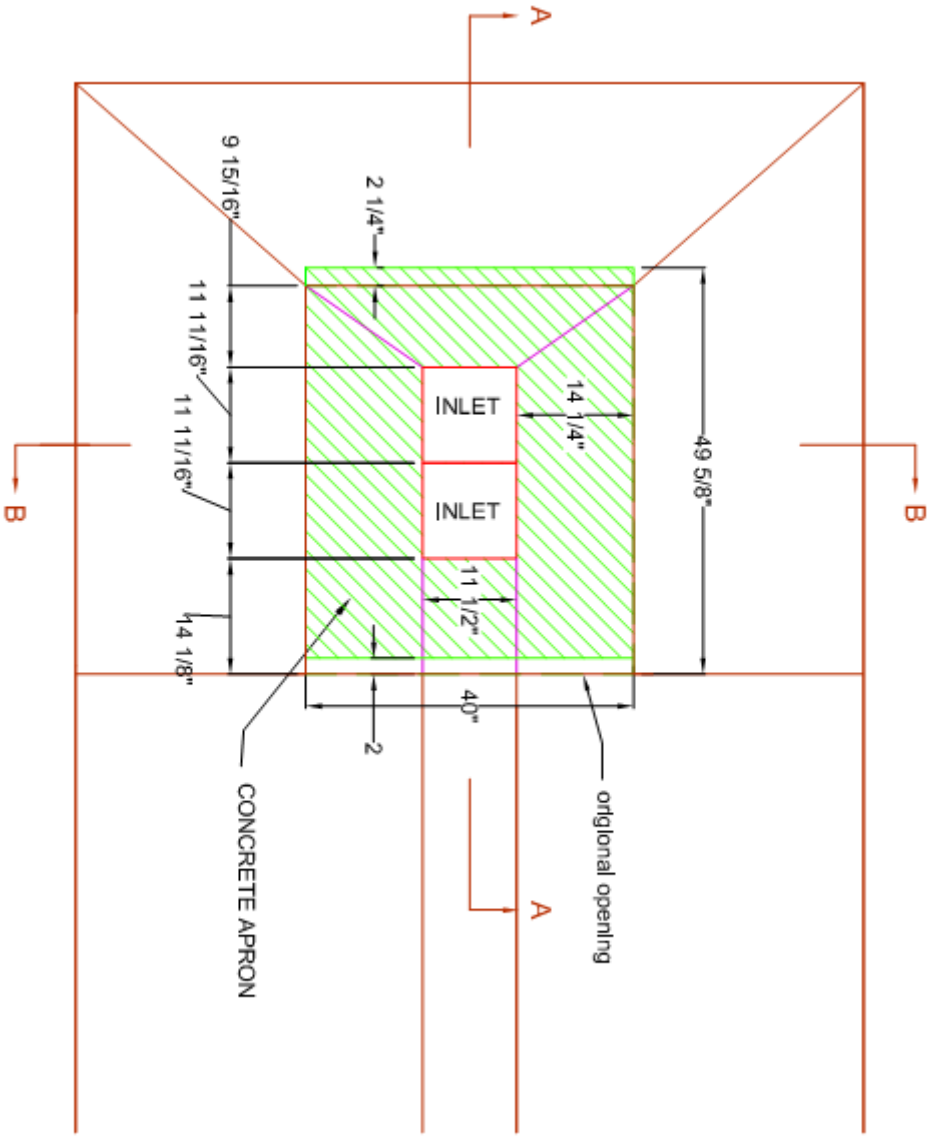

(a) plan view

Figure A-3: Type D inlet schematics

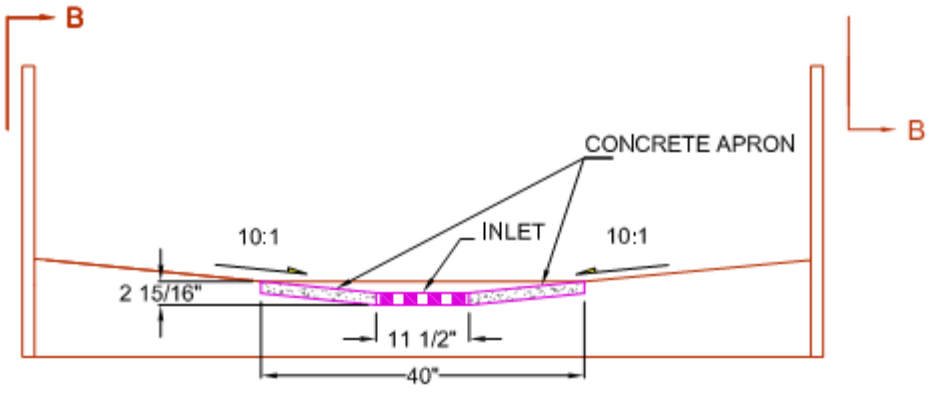

(b) Section B-B

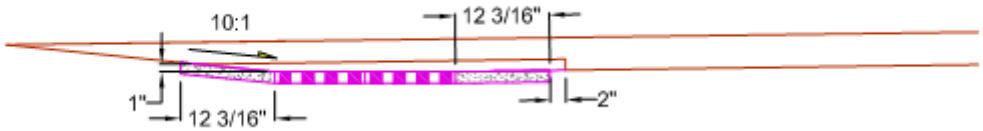

(c) Section A-A

Figure A-3 (continued): Type D inlet schematics

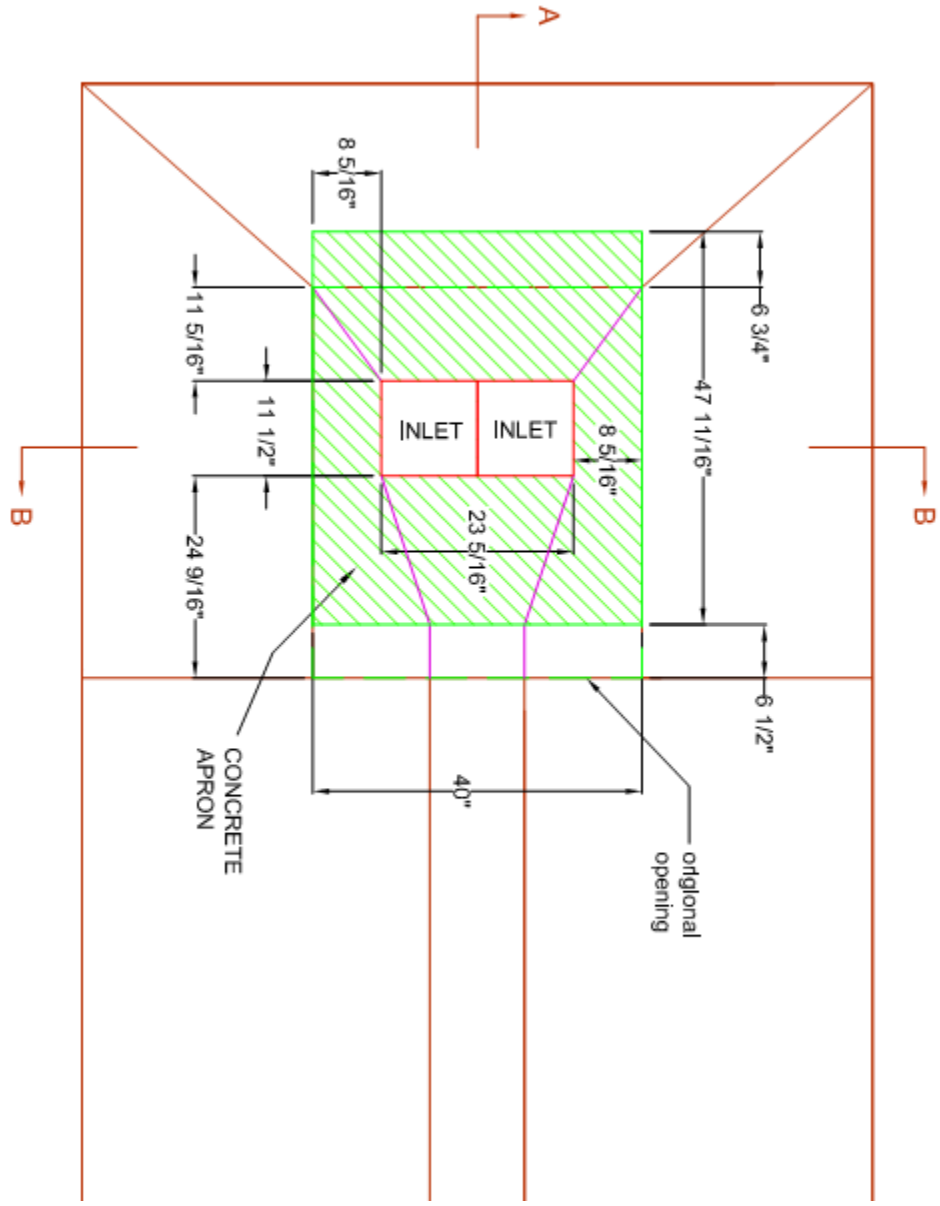

(a) plan view

Figure A-4: Type D inlet rotated schematics

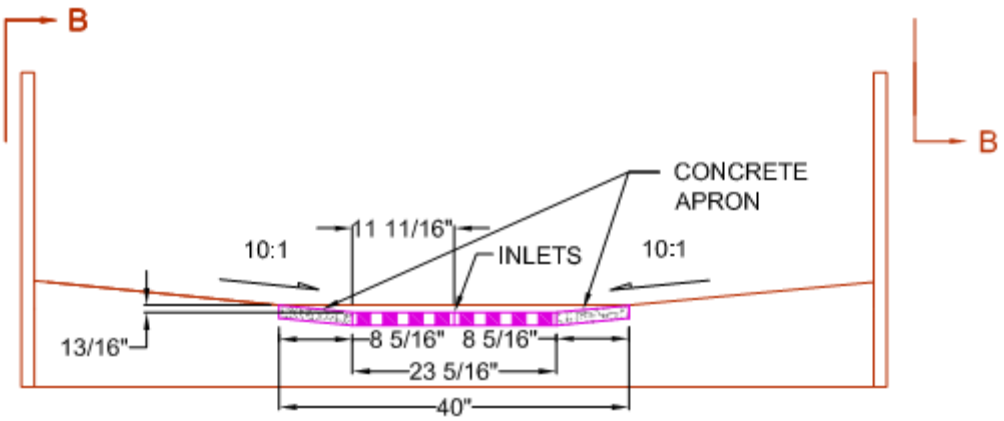

(b) Section B-B

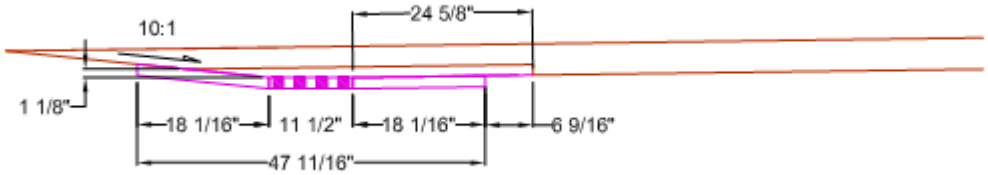

(c) Section A-A

Figure A-4 (continued): Type D inlet rotated schematics

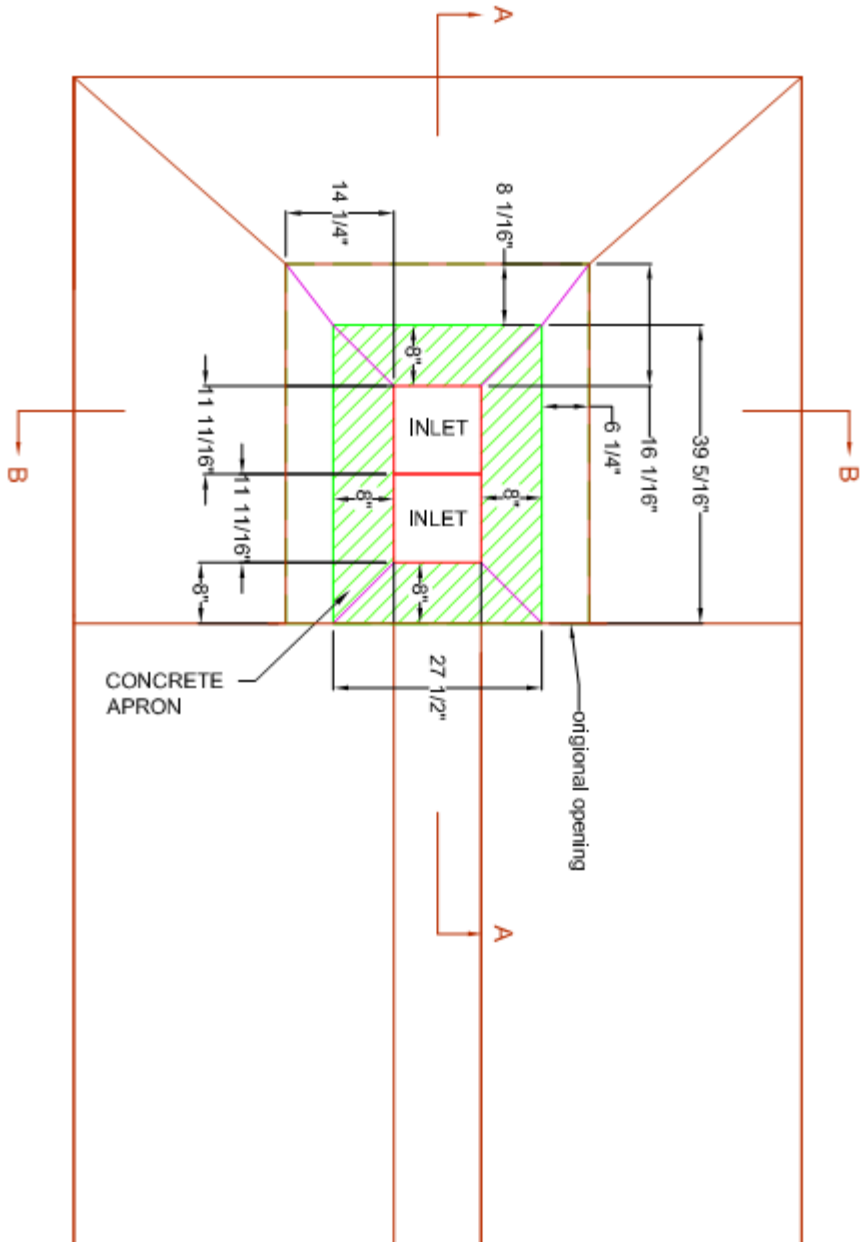

(a) plan view

Figure A-5: Type D inlet depressed schematics

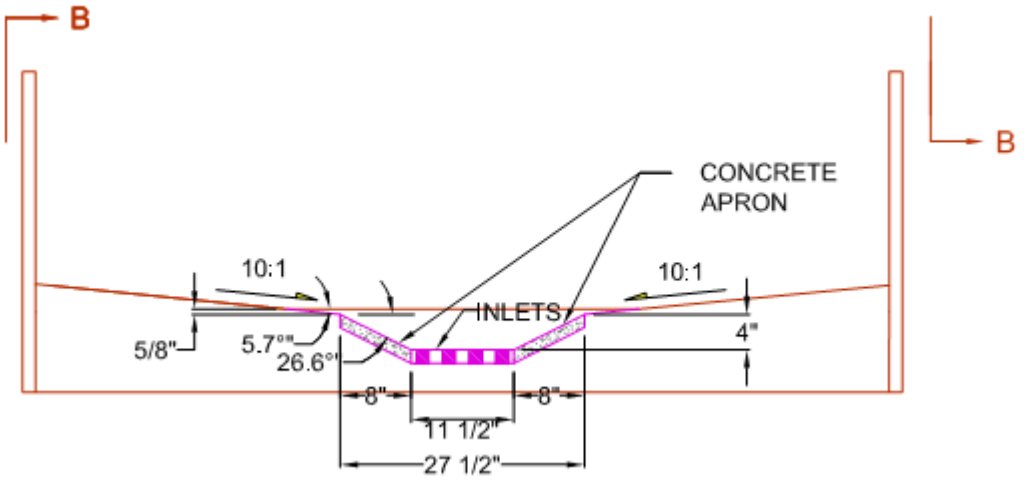

(b) Section B-B

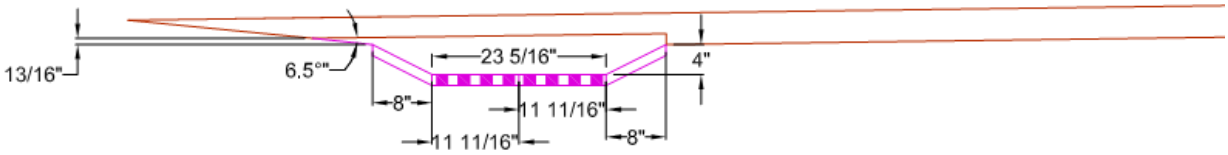

(c) Section A-A

Figure A-5 (continued): Type D inlet depressed schematics

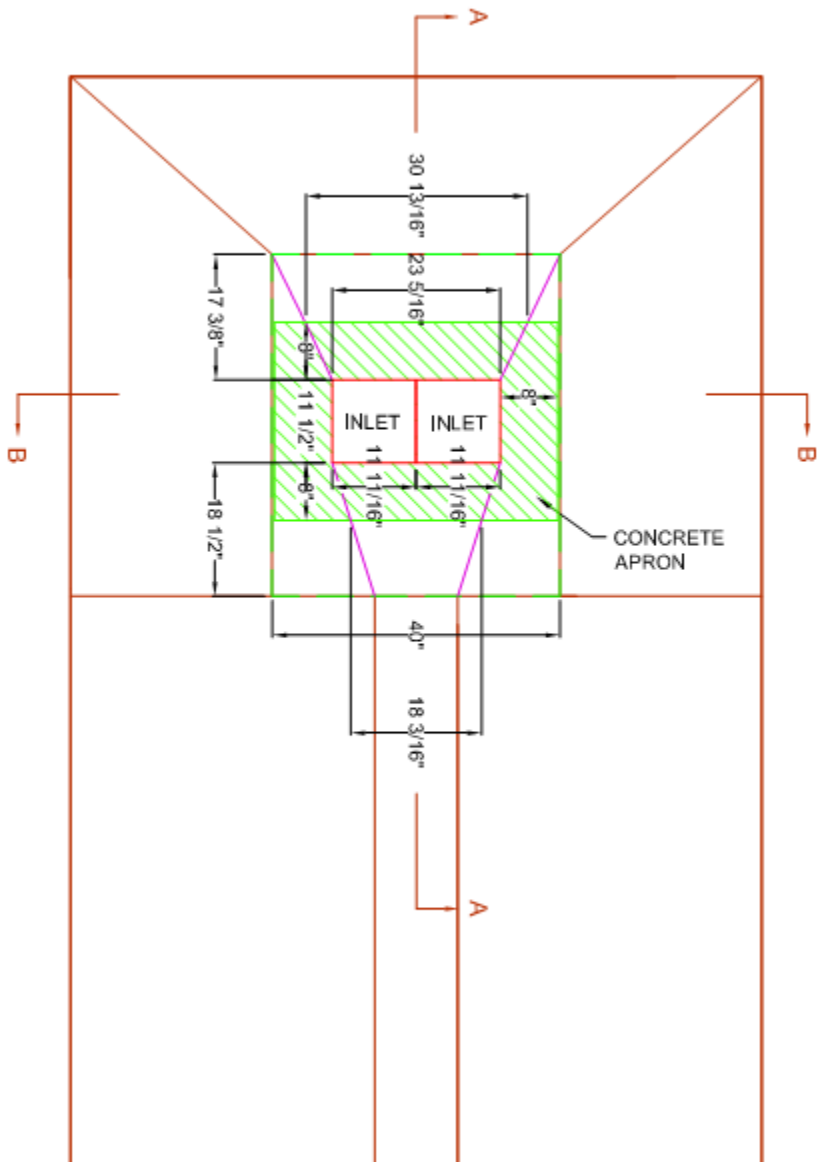

(a) plan view

Figure A-6: Type D inlet rotated and depressed schematics

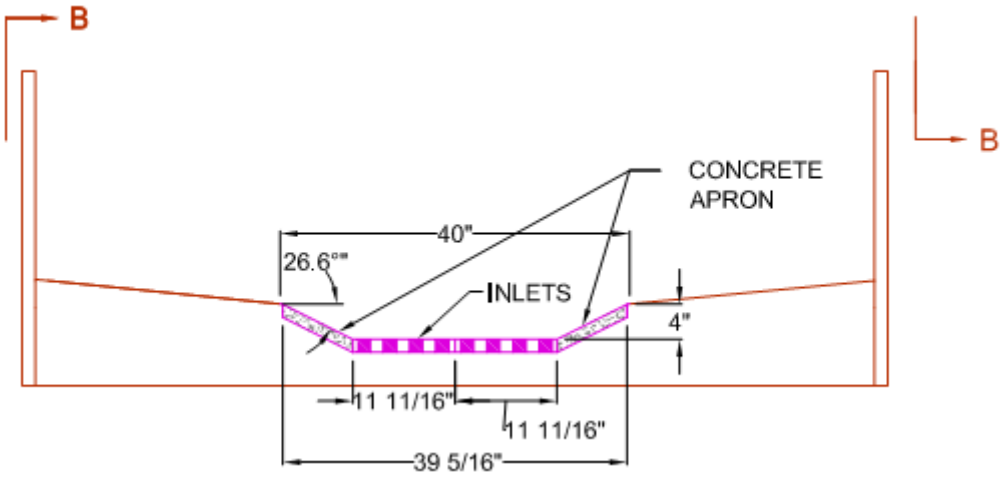

(b) Section B-B

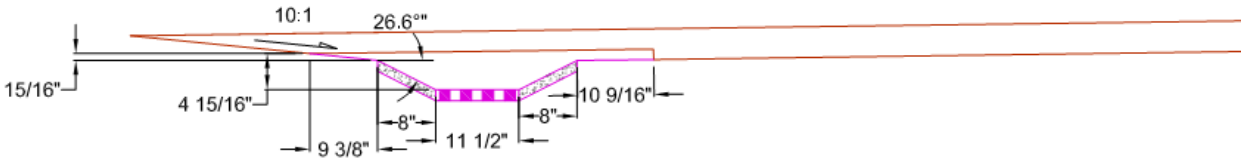

(c) Section A-A

Figure A-6 (continued): Type D inlet rotated and depressed schematics

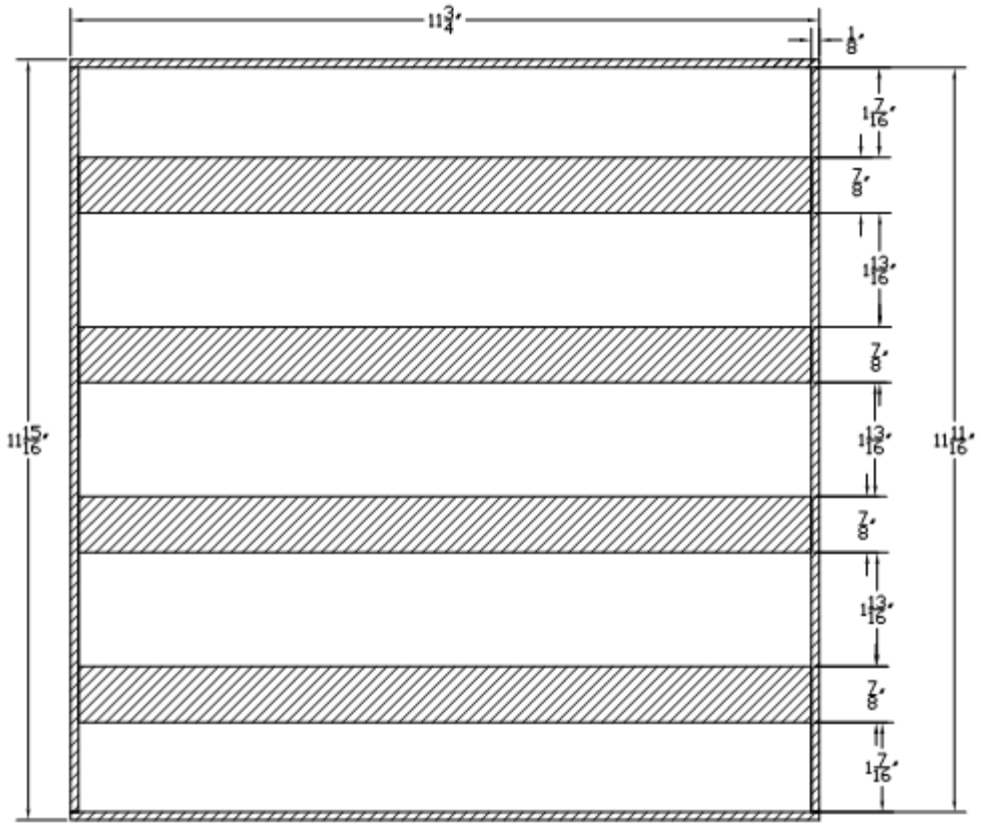

(a) plan view

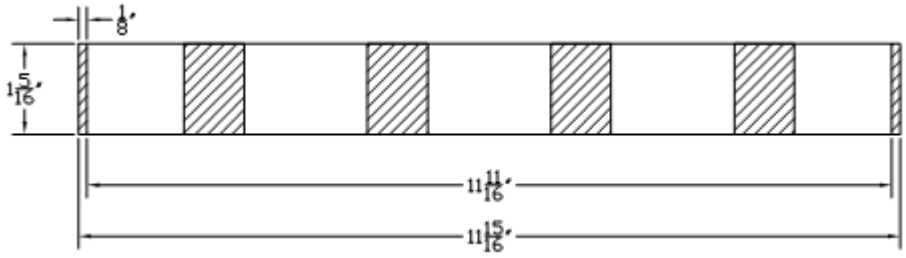

(b) profile view

Figure A-7: Grate schematics

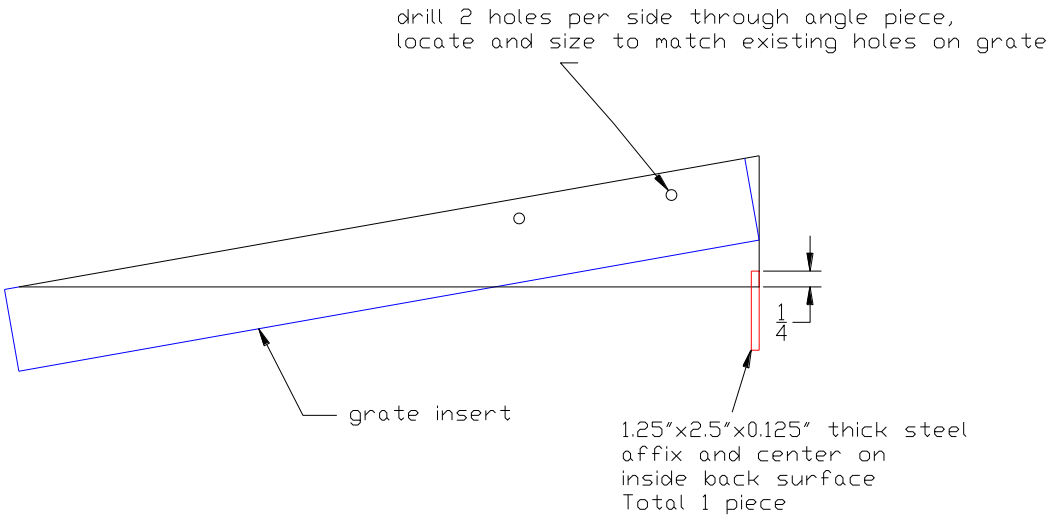

(a) profile view of Type C inlet grate and first upstream grate for Type D inlet

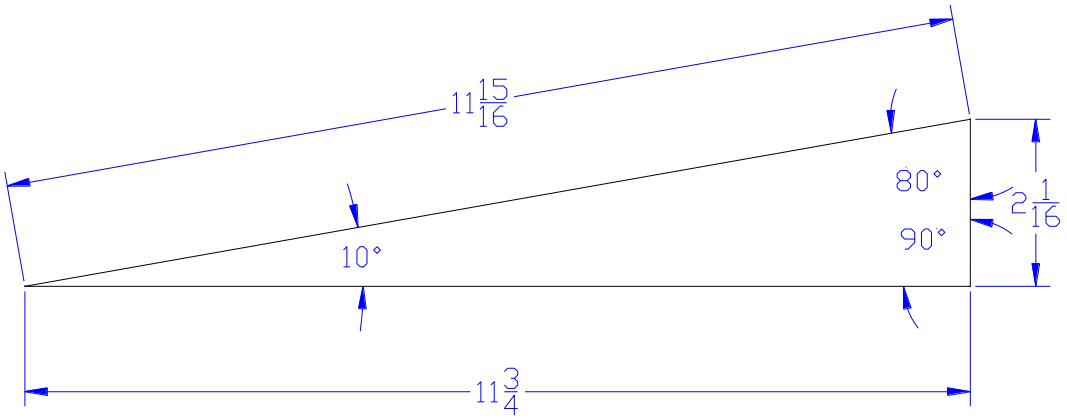

(b) profile view of insert only for Type C inlet grate and first upstream grate for Type D inlet

Figure A-8: 10-degree angled insert schematics

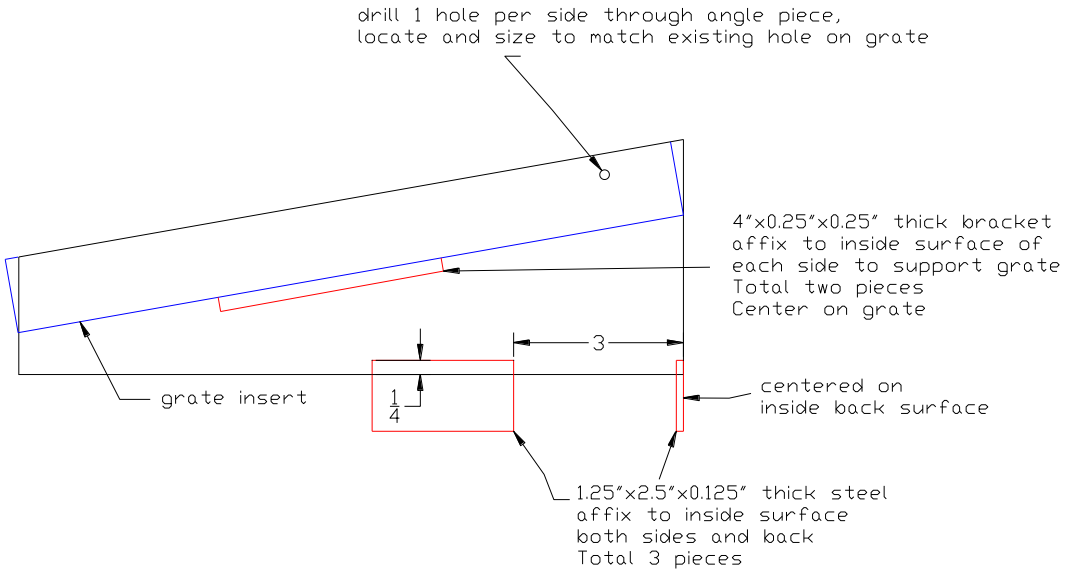

(c) profile view of Type D inlet downstream grate

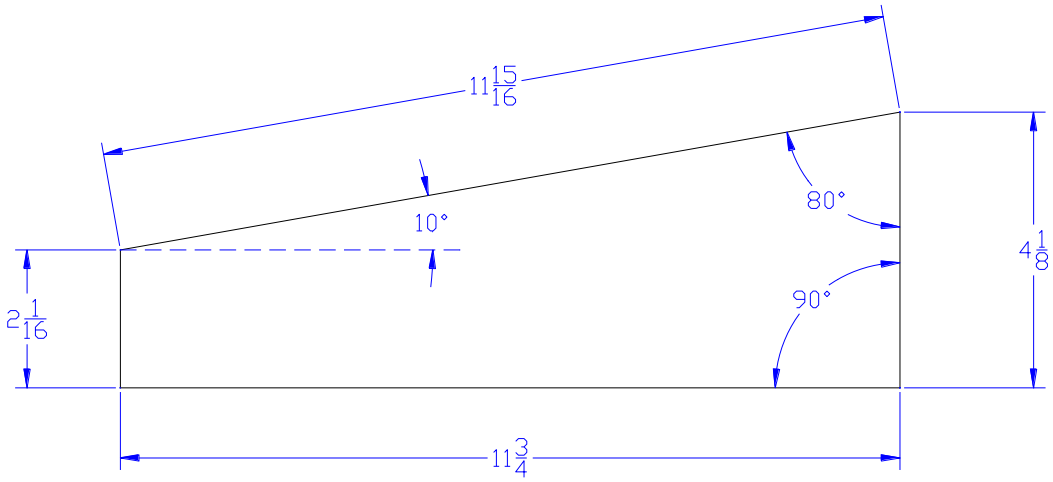

(d) profile view of insert only for Type D inlet downstream grate

Figure A-8 (continued): 10-degree angled insert schematics

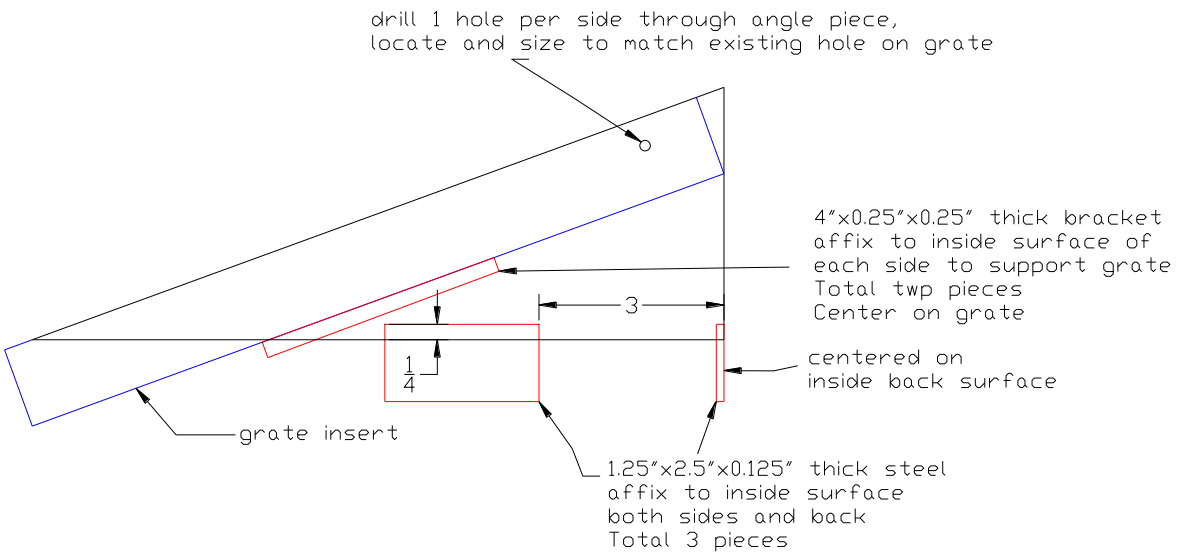

(a) profile view of Type C inlet grate and first upstream grate for Type D inlet

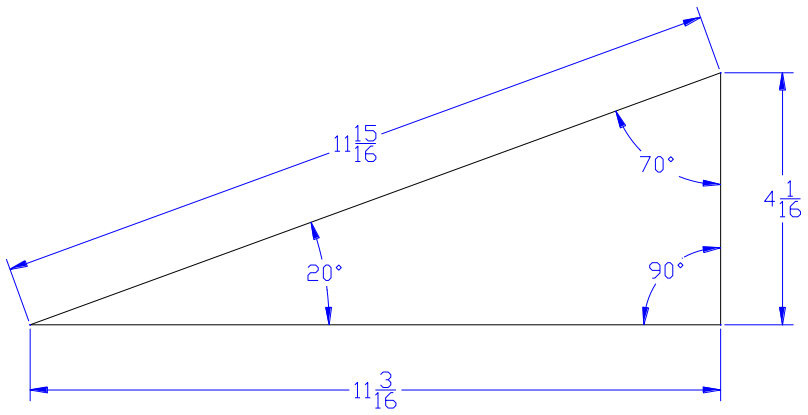

(b) profile view of insert only for Type C inlet grate and first upstream grate for Type D inlet

Figure A-9: 20-degree angled insert schematics

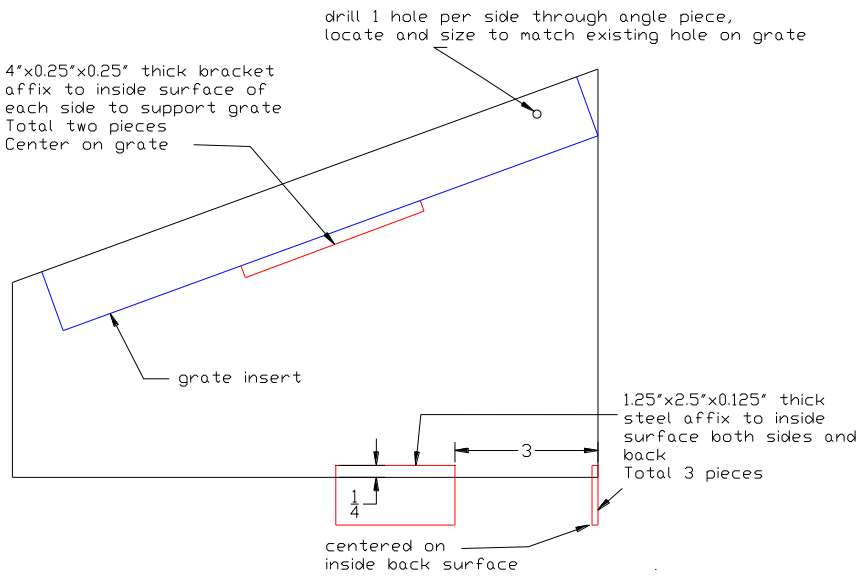

(c) profile view of Type D inlet downstream grate

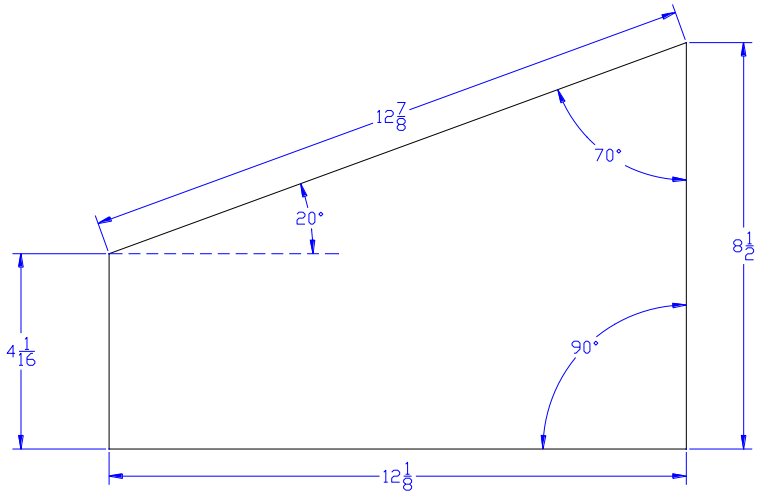

(d) profile view of insert only for Type D inlet downstream grate

Figure A-9 (continued): 20-degree angled insert schematics

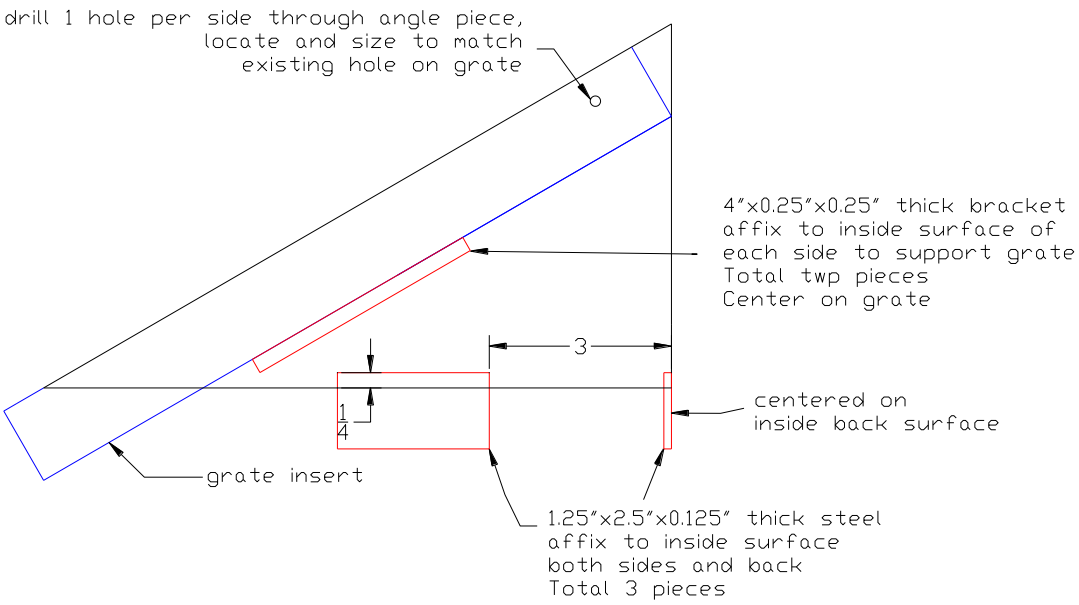

(a) profile view of Type C inlet grate and first upstream grate for Type D inlet

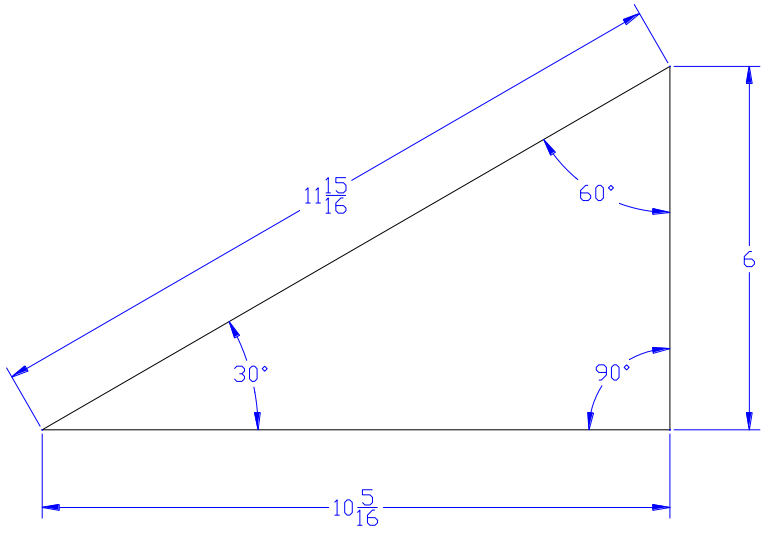

(b) profile view of insert only for Type C inlet grate and first upstream grate for Type D inlet

Figure A-10: 30-degree angled insert schematics

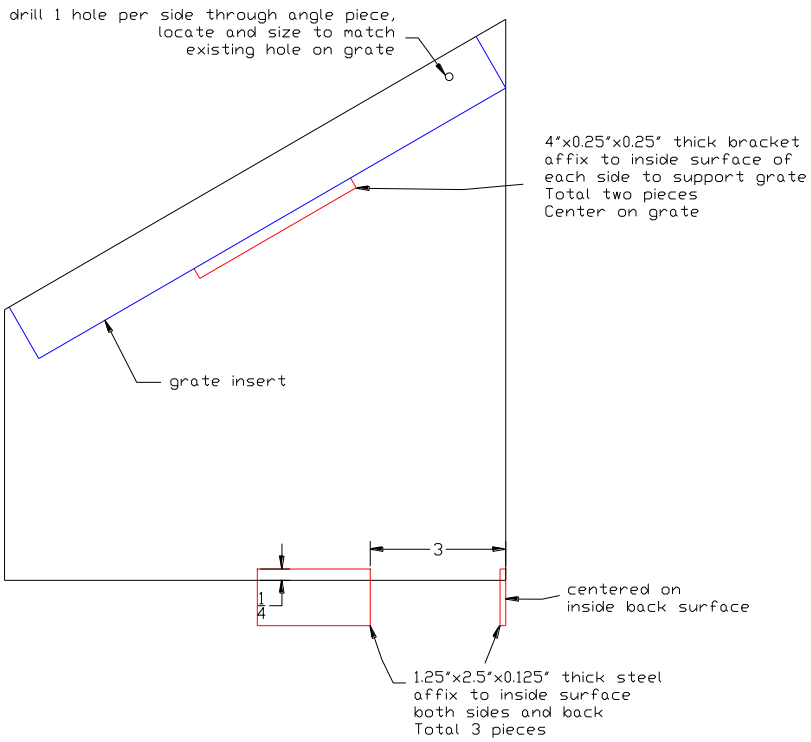

(c) profile view of Type D inlet downstream grate

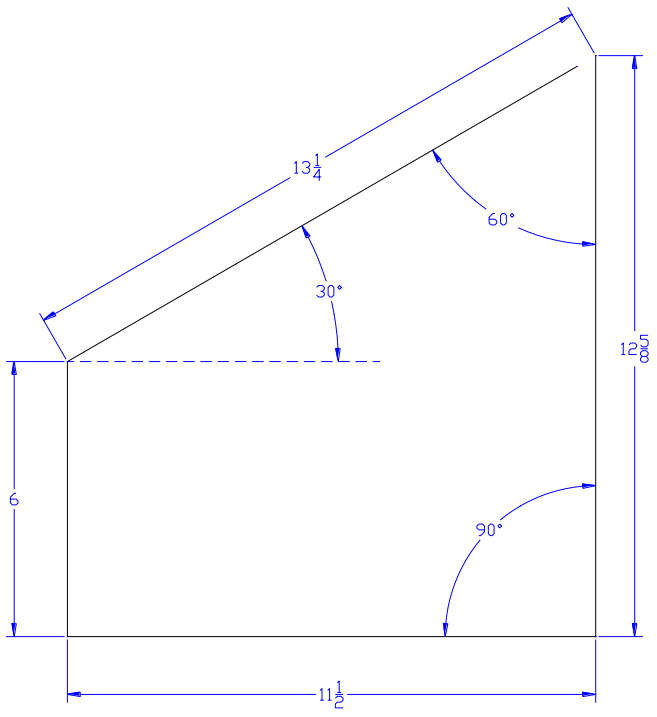

(d) profile view of insert only for Type D inlet downstream grate

Figure A-10 (continued): 30-degree angled insert schematics

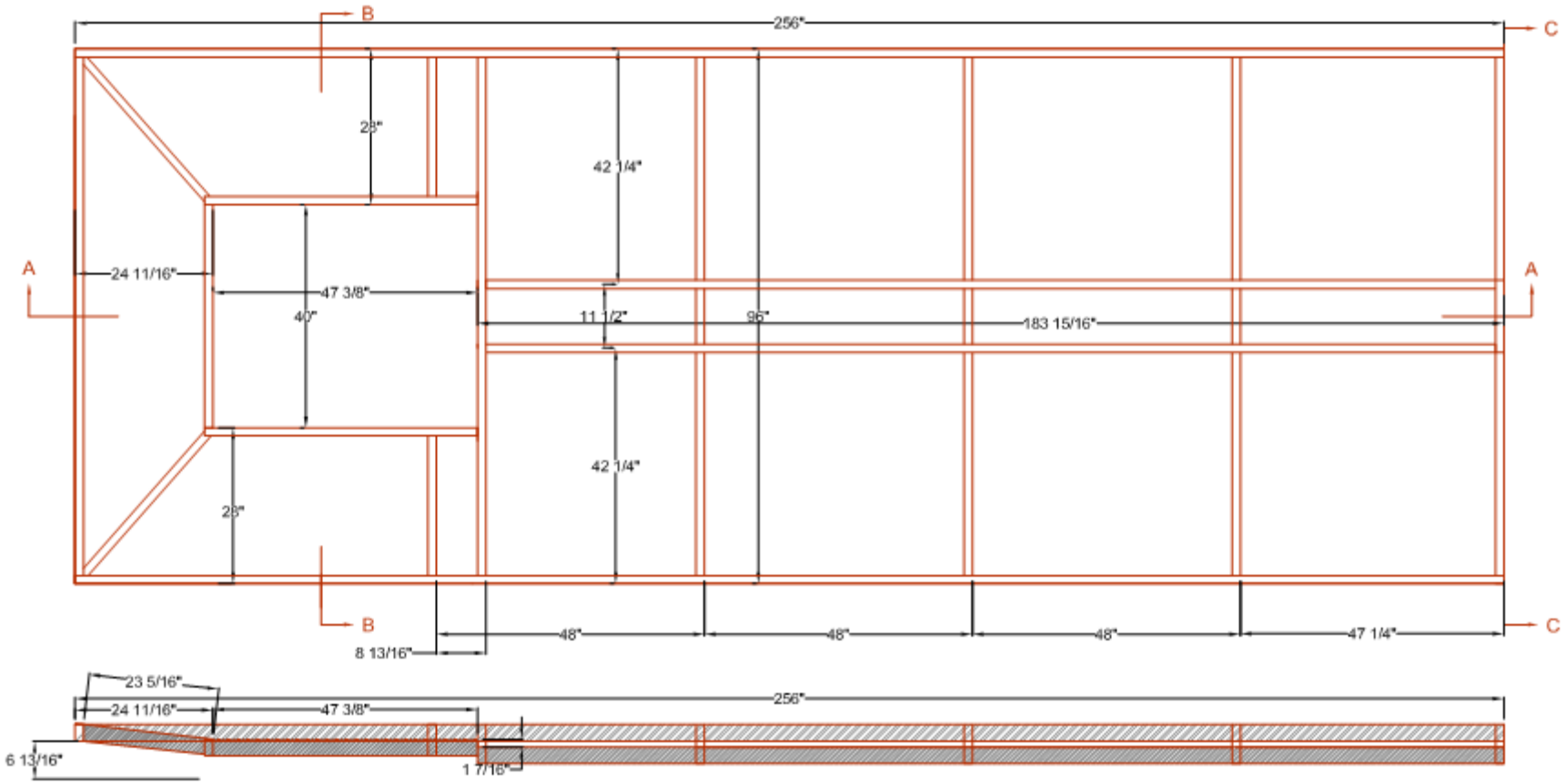

(a) plan view and Section A-A

Figure A-11: Median section schematics

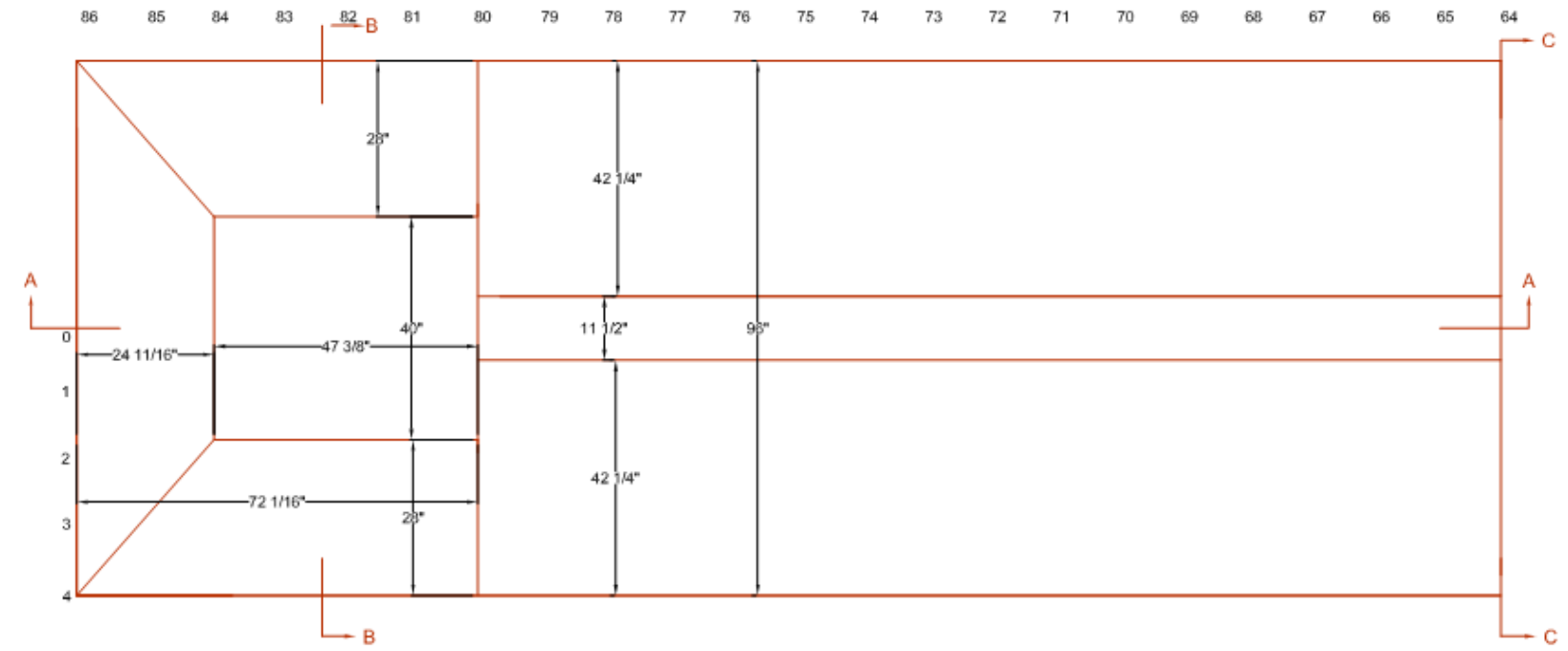

(b) plan view with stationing

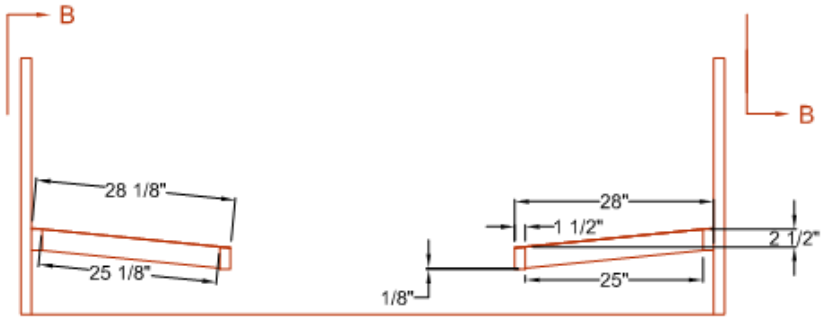

(c) Section B-B

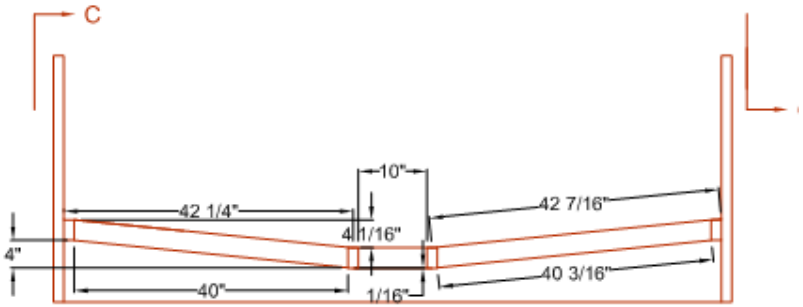

(d) Section C-C

Figure A-11 (continued): Median section schematics

APPENDIX B

TEST DATA

Table B-1: Test data for inlets

Test ID Number	Configuration	Grate Angle (°)	Inlet Depth (ft)	Flow Measured (cfs)	Prototype Inlet Depth (ft)	Prototype Flow (cfs)
1	Type C	0	0.352	1.84	1.06	28.7
2	Type C	0	0.513	2.46	1.54	38.4
3	Type C	0	0.795	3.39	2.39	53.0
4	Type C	0	1.037	3.75	3.11	58.6
6	Type C	10	0.370	1.85	1.11	28.9
7	Type C	10	0.528	2.46	1.58	38.4
8	Type C	10	0.765	3.14	2.30	49.0
9	Type C	10	1.044	3.62	3.13	56.5
11	Type C	20	0.369	1.72	1.11	26.9
12	Type C	20	0.506	2.24	1.52	35.0
13	Type C	20	0.798	2.98	2.39	46.5
14	Type C	20	0.989	3.41	2.97	53.3
16	Type C	30	0.362	1.53	1.09	23.9
17	Type C	30	0.516	2.24	1.55	35.0
18	Type C	30	0.748	2.86	2.24	44.7
19	Type C	30	1.008	3.50	3.02	54.7
21	Type C depressed	0	0.668	1.95	2.00	30.5
22	Type C depressed	0	0.834	2.43	2.50	38.0
23	Type C depressed	0	1.089	3.60	3.27	56.2
24	Type C depressed	0	1.365	4.23	4.10	66.1
26	Type C depressed	10	0.707	1.87	2.12	29.2
27	Type C depressed	10	0.864	2.50	2.59	39.1
28	Type C depressed	10	1.118	3.43	3.35	53.6
29	Type C depressed	10	1.341	4.04	4.02	63.1
31	Type C depressed	20	0.639	2.35	1.92	36.7
32	Type C depressed	20	0.840	2.42	2.52	37.8
33	Type C depressed	20	1.098	3.25	3.29	50.8
34	Type C depressed	20	1.337	3.89	4.01	60.8
36	Type C depressed	30	0.685	2.55	2.06	39.8
37	Type C depressed	30	0.825	2.84	2.48	44.4
38	Type C depressed	30	1.078	3.25	3.23	50.8
39	Type C depressed	30	1.345	3.99	4.04	62.3
41	Type D rotated depressed	0	0.632	4.46	1.90	69.7
42	Type D rotated depressed	0	0.849	3.80	2.55	59.4
43	Type D rotated depressed	0	1.080	5.55	3.24	86.7
44	Type D rotated depressed	0	1.354	7.93	4.06	123.9
46	Type D rotated depressed	10	0.638	4.16	1.91	65.0
47	Type D rotated depressed	10	0.856	3.44	2.57	53.7
48	Type D rotated depressed	10	1.074	5.06	3.22	79.0
49	Type D rotated depressed	10	1.327	7.68	3.98	120.0
51	Type D rotated depressed	20	0.673	4.27	2.02	66.7
52	Type D rotated depressed	20	0.826	3.85	2.48	60.1
53	Type D rotated depressed	20	1.083	5.12	3.25	80.0
54	Type D rotated depressed	20	1.341	6.97	4.02	108.9

Test ID Number	Configuration	Grate Angle (°)	Inlet Depth (ft)	Flow Measured (cfs)	Prototype Inlet Depth (ft)	Prototype Flow (cfs)
56	Type D rotated depressed	30	0.663	4.68	1.99	73.1
57	Type D rotated depressed	30	0.839	4.70	2.52	73.4
58	Type D rotated depressed	30	1.080	5.70	3.24	89.0
59	Type D rotated depressed	30	1.377	7.23	4.13	112.9
61	Type D depressed	0	0.657	4.06	1.97	63.4
62	Type D depressed	0	0.979	4.45	2.94	69.5
63	Type D depressed	0	1.075	5.11	3.23	79.8
64	Type D depressed	0	1.345	7.55	4.04	117.9
66	Type D depressed	10	0.660	3.87	1.98	60.4
67	Type D depressed	10	0.932	4.13	2.80	64.5
68	Type D depressed	10	1.094	5.32	3.28	83.1
69	Type D depressed	10	1.336	6.95	4.01	108.6
71	Type D depressed	20	0.673	3.54	2.02	55.3
72	Type D depressed	20	0.846	4.35	2.54	67.9
73	Type D depressed	20	1.085	5.36	3.26	83.7
74	Type D depressed	20	1.326	6.65	3.98	103.9
76	Type D depressed	30	0.674	3.24	2.02	50.6
77	Type D depressed	30	0.844	4.62	2.53	72.2
78	Type D depressed	30	1.101	5.55	3.30	86.7
79	Type D depressed	30	1.332	6.79	4.00	106.1
81	Type D	0	0.323	2.24	0.97	35.0
82	Type D	0	0.509	3.39	1.53	53.0
83	Type D	0	0.749	5.20	2.25	81.2
84	Type D	0	1.005	6.63	3.02	103.6
86	Type D	10	0.366	2.00	1.10	31.2
87	Type D	10	0.513	3.43	1.54	53.6
88	Type D	10	0.770	4.88	2.31	76.2
89	Type D	10	1.015	6.15	3.05	96.1
91	Type D	20	0.335	1.11	1.01	17.3
92	Type D	20	0.504	2.27	1.51	35.5
93	Type D	20	0.758	4.20	2.27	65.6
94	Type D	20	1.001	5.60	3.00	87.5
96	Type D	30	0.358	1.29	1.07	20.1
97	Type D	30	0.528	2.19	1.58	34.2
98	Type D	30	0.780	3.52	2.34	55.0
99	Type D	30	1.022	4.99	3.07	77.9
101	Type D rotated	0	0.334	2.55	1.00	39.8
102	Type D rotated	0	0.494	2.95	1.48	46.1
103	Type D rotated	0	0.758	4.75	2.27	74.2
104	Type D rotated	0	1.001	6.60	3.00	103.1
106	Type D rotated	10	0.354	2.45	1.06	38.3
107	Type D rotated	10	0.488	2.90	1.46	45.3
108	Type D rotated	10	0.753	4.30	2.26	67.2
109	Type D rotated	10	1.008	6.70	3.02	104.7
111	Type D rotated	20	0.332	2.07	1.00	32.3
112	Type D rotated	20	0.503	3.75	1.51	58.6

Test ID Number	Configuration	Grate Angle (°)	Inlet Depth (ft)	Flow Measured (cfs)	Prototype Inlet Depth (ft)	Prototype Flow (cfs)
113	Type D rotated	20	0.745	4.50	2.24	70.3
114	Type D rotated	20	1.014	6.45	3.04	100.7
116	Type D rotated	30	0.353	2.45	1.06	38.3
117	Type D rotated	30	0.518	3.82	1.55	59.7
118	Type D rotated	30	0.761	5.02	2.28	78.4
119	Type D rotated	30	1.025	6.50	3.08	101.5

Note: Test ID Numbers 5 through 120 (in multiples of 5) denote the twenty-four debris tests and are tabulated in Table B-2.

Table B-2: Debris test data

Test ID Number	Configuration	Grate Angle (°)	Initial Inlet Depth (ft)	Depth Change (ft)	Measured Flow (cfs)	Prototype Inlet Depth (ft)	Prototype Depth Change (ft)	Prototype Flow (cfs)
5	Type C debris	0	0.348	0.219	1.65	1.04	0.66	25.8
10	Type C debris	10	0.353	0.228	1.75	1.06	0.68	27.3
15	Type C debris	20	0.229	0.167	0.9	0.69	0.50	14.1
20	Type C debris	30	0.330	0.140	1.34	0.99	0.42	20.9
25	Type C depressed debris	0	0.670	0.331	1.96	2.01	0.99	30.6
30	Type C depressed debris	10	0.758	0.178	2.05	2.27	0.53	32.0
35	Type C depressed debris	20	0.744	0.241	2.14	2.23	0.72	33.4
40	Type C depressed debris	30	0.681	0.266	2.53	2.04	0.80	39.5
45	Type D rotated depressed debris	0	0.645	0.701	4.5	1.94	2.10	70.3
50	Type D rotated depressed debris	10	0.650	0.551	4.25	1.95	1.65	66.4
55	Type D rotated depressed debris	20	0.661	0.398	4.27	1.98	1.19	66.7
60	Type D rotated depressed debris	30	0.651	0.434	4.37	1.95	1.30	68.3
65	Type D depressed debris	0	0.645	0.720	4.03	1.94	2.16	62.9
70	Type D depressed debris	10	0.662	0.675	3.88	1.99	2.02	60.6
75	Type D depressed debris	20	0.679	0.468	3.59	2.04	1.40	56.1
80	Type D depressed debris	30	0.673	0.481	3.23	2.02	1.44	50.5
85	Type D debris	0	0.325	0.134	2.25	0.98	0.40	35.1
90	Type D debris	10	0.363	0.014	1.94	1.09	0.04	30.3
95	Type D debris	20	0.610	0.085	3.04	1.83	0.25	47.5
100	Type D debris	30	0.805	0.113	3.65	2.42	0.34	57.0
105	Type D rotated debris	0	0.334	0.329	2.59	1.00	0.99	40.5
110	Type D rotated debris	10	0.280	0.155	2.23	0.84	0.46	34.8
115	Type D rotated debris	20	0.332	0.078	2.07	1.00	0.23	32.3
120	Type D rotated debris	30	0.346	0.064	2.2	1.04	0.19	34.4

APPENDIX C

DATA COLLECTION

UDFCD Median Drain Inlet Study Data Sheet

Date: _____ Test ID number: _____
Operators (*first initial and last name*): _____
Start time: _____ End time: _____
Water temperature (ºF): _____

Model Information

Inlet type (*circle one*): Type C Type D
Inlet modification (*circle one*): None Depressed Rotated Rotated depressed
Grate angle (deg) (*circle one*): 0 10 20 30
Other: _____
Debris (*circle one*): Y N Type: _____

Discharge Information

Mag meter reading (cfs): _____ Weir (ft): _____

Depth Readings

(*zero at the front of the first grate; depth readings lateral to the grate center*)
Zero: _____
Depth: _____ _____

Description of Flow into Inlets and Observations

(i.e., Is there a vortex and where over the inlet is it located? For the Type D inlet, which grate has more flow? Where is the flow most turbulent over the grates? etc.)

_____
_____
_____
_____
_____
_____

Extent of Flow

Station (x)	Spread (y)	Notes

ELECTRONIC DATA SUPPLEMENT

CONTENTS AND ORGANIZATION

(stored on a DVD)

Folder	Files and/or Sub-folders
Client Final Report	Microsoft Word® (.doc) and Adobe® Acrobat® (.pdf) files; and SureThing (.std) CD label file
*Data and Photographs**	Type C inlet Type C inlet depressed Type D inlet Type D inlet depressed Type D inlet rotated Type D inlet rotated and depressed

*The reader is referred to the UDFCD for obtaining photographs and video documentation.